Parameters, Calculation of Nuclear Magnetic Resonance

Cynthia J. Jameson

Department of Chemistry M/C-111, University of Illinois at Chicago, Room 4500 Science and Engineering South Building, 845 West Taylor Street, Chicago, Illinois 60607-7061, USA

The fundamental parameters that reproduce a nuclear magnetic resonance (NMR) spectrum in gases, liquids and solids are the four tensor quantities: the NMR chemical shift of the nucleus, the indirect nuclear spin–spin coupling, the nuclear electric quadrupole coupling, and the direct dipolar coupling tensors. The first three are intimately related to the local electronic structure at the nucleus and the chemical bonds connecting the nuclei. On the other hand, the direct nuclear spin dipole–dipole interaction depends directly and entirely on the third power of the inverse of the direct through-space distance between two nuclei, whether bonded or otherwise. In gases and in liquids where free tumbling of the molecules bearing the nuclear spins leads to isotropic averaging of these quantities, only the isotropic average values, the average of three components along the principal axes of the chemical shift and the indirect spin–spin coupling tensors determine the observed frequencies in the NMR spectrum. In the solid state, restricted motion permits the tensors to manifest all the components, whether the sample is a polycrystalline powder, an amorphous solid, or a single crystal. Theoretical calculations of the NMR chemical shift, indirect spin–spin coupling and nuclear quadrupole coupling parameters, using quantum mechanical methods, permit the prediction of NMR spectra

For references see page •••

and provide the physical basis for the relationship between the parameters and molecular electronic structure, which may include local electronic structure (electronic distribution in the immediate vicinity of the nucleus and neighboring bonds), local molecular geometry, bond connectivities, stereochemical structure, as well as subtle effects of the chemical environment, such as contributions from remote parts of the molecule, tertiary and secondary structure, crystal packing, solvent effects, and isotopic substitution.

1 INTRODUCTION

The fundamental parameters that reproduce a NMR spectrum in gases, liquids and solids are: the NMR chemical shift of the nucleus, the indirect nuclear spin–spin coupling, and the nuclear quadrupole coupling. All three quantities are tensors whose directional properties are intimately related to the local electronic structure at the nucleus. In gases and in liquids where free tumbling of the molecules bearing the nuclear spin leads to isotropic averaging of these quantities, only a single number determines the frequencies in the NMR spectrum: the isotropic average value, the average of three components along the principal axes of the tensor. In the solid state, restricted motion permits the tensors to manifest all the components, whether the sample is a polycrystalline powder, an amorphous solid, or a single crystal.

There is a fourth parameter which is just as important, the direct nuclear spin dipole–dipole interaction, which depends directly and entirely on the third power of the inverse of the distance between two nuclei, whether bonded or otherwise, and irrespective of the electronic structure. It is a very important parameter in the solid state because it depends on structure, and for protons in a large molecule in solution, it provides the nuclear Overhauser effect (NOE) at intensities which makes it possible to elicit geometrical structure of the nonfloppy parts of the molecule. This direct dipole–dipole interaction parameter is not considered in the theoretical calculations described here because of the trivial mathematical relationship between the parameter and the direct through-space distance.

1.1 Absolute Shielding Tensor and Nuclear Magnetic Resonance Chemical Shift

The NMR spectrum provides the chemical shift δ relative to a chosen reference substance in a chosen medium. The definition of the chemical shift, usually expressed in ppm, Q2 is given in Equation (1)

$$\delta \equiv (\nu - \nu_{\text{ref}})/\nu_{\text{ref}} \tag{1}$$

where ν is the resonance frequency for the nucleus of interest in the sample and ν_{ref} is the resonance frequency for the reference. The resonance frequency is determined by a fundamental molecular electronic property called the nuclear magnetic shielding, σ, which is defined by the Hamiltonian for the energy of a single nucleus N possessing a nuclear magnetic moment $\boldsymbol{\mu}_N$, in an external magnetic field $\mathbf{B}$, Equation (2) (where Z stands for Zeeman and CS stands for Chemical Shift)

$$\mathcal{H}_{Z+CS} = -\boldsymbol{\mu}_N \cdot (1 - \sigma) \cdot \mathbf{B} \tag{2}$$

The magnetic field experienced by the nucleus at its site is different from the applied magnetic field $\mathbf{B}$ because of the small field $\mathbf{B}_{\text{local}}$ arising from the circulations of the electrons induced by the external magnetic field, Equation (3)

$$(\mathbf{B}_{\text{local}})_\alpha = (1 - \sigma)_{\alpha\beta} \cdot \mathbf{B}_\beta, \qquad \alpha, \beta = x, y, z \tag{3}$$

Thus, Equation (4)

$$\mathcal{H}_{CS} = +\boldsymbol{\mu}_N \cdot \sigma \cdot \mathbf{B} \tag{4}$$

The term "magnetic shielding" implies that the magnetic dipole of a nucleus at that site would be shielded from the full effect of the external field by the influence of the induced electronic motions. For free atoms σ is always positive because this circulation generates a shielding field which opposes the applied field. In a molecule the presence of other nuclei hinders this circulation to an extent that depends on the electronic distribution and may even lead to a negative σ. Depending on the symmetry of the electronic distribution at the nuclear site, some of the components $\sigma_{\alpha\beta}$ may be zero or identical. For example, for a linear molecule there are only two unique components, σ_{zz} and σ_{xx}, where z is along the molecular axis; these components are designated as $\sigma_\parallel$ and $\sigma_\perp$, respectively.

Theoretical calculations of the nuclear magnetic shielding provide the entire shielding tensor σ on an absolute basis, i.e. with respect to a bare nucleus. The chemical shift δ expresses a difference in nuclear magnetic shielding, Equation (5)

$$\delta \equiv (\nu - \nu_{\text{ref}})/\nu_{\text{ref}} = (\sigma_{\text{ref}} - \sigma)/(1 - \sigma_{\text{ref}}) \tag{5}$$

Usually, though not always, σ_{ref} can be neglected relative to 1.0, so sometimes it is sufficient to use, Equation (6)

$$\delta \approx (\sigma_{\text{ref}} - \sigma) \tag{6}$$

A *negative chemical shift* means that the nucleus located at site A sees a more shielded (smaller) magnetic field than does the nucleus in the reference substance, so that the *applied field has to be made higher* in order to achieve resonance with the nuclear spin energy separation at site A.

We see from Equation (2) that the mathematical terms in the total energy of a molecule that are bilinear in the external homogeneous magnetic field **B** and the nuclear magnetic moment μ determine the nuclear magnetic shielding σ for a nucleus in a molecule. The theoretical calculation of NMR chemical shifts from first principles therefore consists of collecting all such bilinear terms in the energy of a molecule in the presence of both an external magnetic field and a nuclear magnetic moment located at the observed site to obtain the absolute shielding tensor quantities σ. A separate calculation is required for the reference molecule. The NMR chemical shift tensor can then be calculated from differences between σ and σ_{ref}.

1.2 Indirect Spin–Spin Coupling Tensor

Usually, more than one nuclear spin is present in the observed molecule. The interaction of nuclear spins N and N′ is composed of a direct through-space dipolar coupling (coupling of the bare nuclear magnetic dipole moments) and an indirect interaction by way of the electrons. The Hamiltonian for this interaction energy is, Equation (7)

$$\mathcal{H}_{D+J} = \mu_N \cdot (\mathbf{D} + \mathbf{J}) \cdot \mu_{N'} \tag{7}$$

The direct dipolar coupling tensor **D** is symmetric with the principal components summing to zero (a traceless tensor), and depends entirely on the distance vector between N and N′. In an oriented system both **D** and **J** (the spin–spin coupling) contribute to the observed spectrum. In a rapidly tumbling molecule in solution, only the isotropic average of **J** survives ($\mathbf{J}_{iso} = (1/3)[\mathbf{J}_{xx} + \mathbf{J}_{yy} + \mathbf{J}_{zz}]$); the anisotropic part averages to zero. A *positive* **J** results from an interaction which minimizes the energy when the two nuclear spins are *antiparallel*. Theoretical calculations of the **J** tensor from first principles consists of collecting all such bilinear terms in the energy of a molecule, as shown in Equation (7).

1.3 Electric Field Gradient Tensor and Nuclear Quadrupole Coupling Constant

All nuclei with spin $I > 1/2$ have an ellipsoidal distribution of charge and an electric quadrupole moment eQ, where e is the magnitude of the charge of an electron. Q is positive if the nucleus is prolate (cigar-like), negative if oblate (pancake-like). Q is an intrinsic property of the nucleus. Energy is minimized by appropriate alignment of an electric quadrupole in an electric field gradient. At a nuclear site in a molecule, there is an electric field gradient when there is an asymmetry in the charge distribution due to the electrons and other nuclei. This electric field gradient is represented by $e\mathbf{q}$. The energy of a nuclear quadrupole is quantized according to its orientation in the electric field gradient, even in the absence of an external magnetic field. The electrostatic energy of interaction between the electric quadrupole moment and the electric field gradient is expressed in terms of the nuclear quadrupole coupling constant ($e^2Qq_{zz}/\hbar$).

The magnetic dipole moment of a quadrupolar nucleus is along the axis of symmetry of the nuclear charge distribution. Thus, when a quadrupolar nucleus is placed in a magnetic field so that the nuclear magnetic dipole tends to align with the external magnetic field, the interaction of the electric quadrupole with the internal electric field gradient at the nuclear site in the molecule affects the nuclear magnetic energy levels. The tensor coupling between the nuclear spin and the electric field gradient $e\mathbf{q}$ at the nucleus is described by the Hamiltonian, Equation (8)

$$\mathcal{H}_Q = \mathbf{I}_N \cdot (eQ/2I(2I-1))e\mathbf{q} \cdot \mathbf{I}_{N'} \tag{8}$$

Like **D**, the electric field gradient tensor is traceless: the isotropic average of energy terms involving **q** is zero. Thus, in liquids or gases the positions of the lines in the NMR spectrum are not affected by the nuclear quadrupole coupling. In solids the nuclear quadrupole coupling can dominate the NMR spectrum and measurements of the nuclear quadrupole coupling tensor in single crystals or powders provide the electric field gradient tensors.

1.4 Nuclear Magnetic Resonance Parameters in Gases, Liquids, and Solids

In gases and liquids, isotropic averaging caused by the rapid tumbling of molecules leads to observations of only the isotropic part of σ and **J**, which are given by one third the sum of the principal components of these tensors. At the same time, **D** and **q** being traceless means that this sum is zero. Thus, in liquids or gases the positions of the lines in the NMR spectrum are not affected by either the direct dipolar coupling or the nuclear quadrupole coupling. To a good approximation, neither the chemical shift nor the spin–spin coupling **J** is dependent on the strength of the magnetic field. Actually, one has to be quite specific in defining the environment of the nucleus in both sample and reference because the NMR chemical shift is very sensitive to these. For example, the chemical shift of a ^{13}C nucleus in molecule A relative to the usual reference, tetramethylsilane (TMS) is $\delta_A = \sigma(^{13}C, \text{in TMS, in } CDCl_3 \text{ solution}, x_A, x_{TMS}, x_{CDCl_3}, 300\,K) - \sigma(^{13}C, \text{in A, in } CDCl_3 \text{ solution}, x_A, x_{TMS}, x_{CDCl_3}, 300\,K)$.

It is important to specify completely all the variables (e.g. mole fractions x_A, etc.) that determine the observed chemical shift because the nuclear magnetic shielding is so sensitive to factors of molecular structure and environment. There is an intrinsic mass and temperature dependence of the chemical shift, the spin–spin coupling,

For references see page •••

and the nuclear quadrupole coupling because all three are functions of the electron distribution, which in turn is a function of the nuclear positions. As the internuclear separations are weighted according to the vibrational functions, the thermal average values of these NMR parameters are dependent on the vibrational and rotational state populations. Furthermore, all three NMR parameters are dependent on the medium since each one is affected by the electronic environment, and the electron distribution is affected by intermolecular interactions and external electric fields. For protons the medium effects are generally small, whereas they can be quite large for other nuclei.

In oriented molecules, such as in liquid crystal solutions, polycrystalline powders, single crystals, or amorphous powders, the tensor nature of the three NMR parameters manifest themselves in the spectrum. In principle, one can measure both the anisotropy and asymmetry of the **J** tensor in rigid solids. However, the anisotropy of **J** transforms similarly to the direct dipolar coupling, thus the two interactions cannot be easily separated via experiment. The anisotropy in **J** is predicted to become more important for coupling constants involving heavier nuclei, whereas **D** depends only on the internuclear distance. Rapid magic-angle spinning (MAS) can be used to obtain high resolution spectra of solids by removing the effects of the anisotropic terms, which in general have a $P_2(\cos\theta)$ dependence. The angle for which $(3\cos^2\theta - 1)$ equals zero is the magic-angle 54.74°. The terms that give rise to the NMR spectrum of quadrupolar nuclei include in addition, a $P_4(\cos\theta)$ dependence. Various techniques have been used to separately determine these three NMR tensors separately from experiment, including the orientations of their principal axis systems. In solids, the spinning sidebands observed in slow MAS NMR spectra arising from tightly **J**-coupled spin pairs contain valuable information about NMR parameters such as the orientation of chemical shift tensors and the sign of **J**. Multidimensional NMR spectra in solids permit the separate determination of the isotropic chemical shifts and the anisotropic line shapes that contain chemical shift tensor and quadrupole coupling information for each site.

Thus, we have seen that the parameters of an NMR spectrum are related to fundamental molecular electronic properties: the chemical shift is related to nuclear magnetic shielding σ and the nuclear quadrupole coupling is related to the electric field gradient tensor $e\mathbf{q}$. The indirect spin–spin coupling **J** is itself a molecular electronic property. Therefore, the general approach to the theoretical calculations of these NMR parameters is through a quantum mechanical calculation of molecular electronic properties in the isolated molecule. Any medium effects that have to be included, when they are large enough, require in addition, ensemble averages for a gas, liquid, or solution. The calculation of the electric field gradient is simplest, since this is a property of the unperturbed electronic state of the molecule. Since σ and **J** are electronic properties associated with the presence of magnetic fields and fields generated by nuclear magnetic moments, their calculation requires the general approaches that apply to multiple perturbations. Furthermore, since the probe nucleus senses electronic environments in the immediate vicinity of the nucleus, high level calculations that take into account electron correlation have to be used for all three parameters to achieve accuracy and relativistic corrections are sometimes necessary. Density functional methods have been very successful and can compete favorably with ab initio calculations.

2 GENERAL THEORETICAL METHODS

The mechanisms by which a nuclear magnetic moment interacts with the molecular field and with external magnetic or electric fields in the ground vibronic state were originally articulated in fundamental work by Ramsey.[1–3] For a unified approach to molecular electronic properties which explicitly shows where the contributing terms arise and thereby also permits the relationships between electronic properties to be perceived, consult the articles by Michelot.[4,5] The complete molecular Hamiltonian in the presence of external magnetic and electric fields, including all relevant interaction terms involving nuclear magnetic moments (such as interaction between the nuclear magnetic moment and the field induced at the nucleus by the molecular motion, as well as those related to the interaction of the magnetic moment induced by this molecular motion with an external magnetic field), treats electrons and nuclei as Dirac particles. Relativistic effects are included from the beginning and effects due to the finite dimensions of nuclei are also taken into account, so that the nuclear quadrupole coupling is a natural outcome.[4] Using this Hamiltonian with relativistic corrections for a free molecule in a nondegenerate electronic state, a second order calculation in degenerate perturbation theory leads to the explicit expressions for the contributing terms to nuclear magnetic shielding σ, indirect spin–spin coupling **J**, nuclear electric quadrupole coupling, and all other molecular electronic properties.[5]

2.1 Multiple Perturbation Theory

All the terms in the molecular Hamiltonian given by Michelot[4] may be treated as perturbations added to a zeroth order part (the kinetic energy of the electrons together with the total coulomb potential energy of all the electrons and nuclei, assumed to have already been solved). These include terms bilinear in $\boldsymbol{\mu}_N$ and **B**. In first order, these will lead to energy terms that are of the form

given by Equation (4), providing the formal expression for the so-called diamagnetic part of the nuclear magnetic shielding σ. In second order, the terms in the molecular Hamiltonian that are linear in μ_N together with those linear in **B** will lead to energy terms that are also of the form given by Equation (4), providing the formal expression for the so-called paramagnetic part of the nuclear magnetic shielding σ. Michelot's expression[5] derived for nuclear magnetic shielding σ reduces to that given by Ramsey[1,2] if the origin of the molecular frame is placed at the center of the nucleus of interest, the orientation being that of the Eckart frame. Formally, the shielding term for nucleus N is given by Equation (9):

$$\begin{aligned}\sigma_{\alpha\beta}(\mathrm{N}) = {} & (\mu_0 e^2/8\pi m)\langle 0|\sum_k\{(\boldsymbol{r}_{k\mathrm{N}}\cdot\boldsymbol{r}_{k0})r_{k\mathrm{N}}^{-3}\delta_{\alpha\beta} \\ & -(r_{k\mathrm{N}}^{\alpha}r_{k0}^{\beta})r_{k\mathrm{N}}^{-3}\}|0\rangle \\ & -(\mu_0 e^2/8\pi m^2)\sum_{n\neq 0}({}^1E_n - E_0)^{-1} \\ & \times\left\{\langle 0|\sum_k r_{k\mathrm{N}}^{-3}L_{k\mathrm{N}}^{\alpha}|n\rangle\langle n|\sum_j L_{j0}^{\beta}|0\rangle\right. \\ & \left.+\langle 0|\sum_j L_{j0}^{\beta}|n\rangle\langle n|\sum_k r_{k\mathrm{N}}^{-3}L_{k\mathrm{N}}^{\alpha}|0\rangle\right\} \qquad (9)\end{aligned}$$

The first index $\alpha(=x,y,z)$ is associated with the nuclear magnetic moment and the second index $\beta(=x,y,z)$ is associated with the external magnetic field. L_{j0}^{β} is the β component of the orbital angular momentum operator for the jth electron with respect to the chosen origin (so-called gauge origin) and $\boldsymbol{r}_{k0}$ is the distance vector between the kth electron and the origin. $L_{k\mathrm{N}}^{\alpha}$ is the α component of the orbital angular momentum operator for the kth electron with respect to the nucleus N as origin. $\boldsymbol{r}_{k\mathrm{N}}$ is the distance vector between the kth electron and the nucleus N. m and e are the mass and charge of the electron, μ_0 is the magnetic permeability of a vacuum. E stands for the energy at states 0 and n (0 is the lowest state and n is an index that runs through all the states of the molecule). In Equation (9) the second term in the expression for $\sigma_{\alpha\beta}(\mathrm{N})$, the paramagnetic term, is written in the so-called sum over states (SOS) form, that is, in terms of the sum $\sum_n$ over all excited states designated by the symbol $|n\rangle$. In the symbol $\langle 0|\sum_k r_{k\mathrm{N}}^{-3}L_{k\mathrm{N}}^{\alpha}|n\rangle$ the operators for the angular momentum and the distance vector for the electrons are integrated over the ground state $\langle 0|$ and the excited state $|n\rangle$.

In the same way, the terms in the molecular Hamiltonian that are bilinear in μ_N and $\mu_{N'}$ lead to the energy terms that are already of the form given by Equation (7) give rise to the first order part of the indirect spin–spin coupling **J**, usually denoted by $\mathbf{J}^{(1a)}$. The terms linear in μ_N in the molecular Hamiltonian in the nonrelativistic limit are three, labeled orbital, spin dipolar (SD) and Fermi contact (FC). In second order, products of these lead to various contributions to the spin–spin coupling **J**. The product of orbital terms lead to $\mathbf{J}^{(1b)}$, $\mathbf{J}^{(1a)}$ is sometimes called the diamagnetic orbital (OD) contribution or $\mathbf{J}^{(\mathrm{OD})}$, and $\mathbf{J}^{(1b)}$ the paramagnetic orbital (OP) contribution or $\mathbf{J}^{(\mathrm{OP})}$ because of the analogy with the diamagnetic and paramagnetic parts of the shielding tensor. The product of SD terms leads to $\mathbf{J}^{(2)}$ or $\mathbf{J}^{(\mathrm{SD})}$, and the product of FC terms leads to $\mathbf{J}^{(3)}$ or $\mathbf{J}^{(\mathrm{FC})}$. By symmetry, there is only one nonvanishing cross-term, resulting from the product of the SD and the contact terms, referred to as $\mathbf{J}^{(4)}$. $\mathbf{J}^{(\mathrm{FC})}$ is purely scalar (isotropic), whereas the others are anisotropic. The motional average of $\mathbf{J}^{(4)}$ is zero, thus, all but $\mathbf{J}^{(4)}$ contribute to the observed isotropic average spin–spin coupling for a rapidly tumbling molecule in solution. All terms contribute to the observed NMR spectrum in solids. The formal expressions for spin–spin coupling in the nonrelativistic limit are shown below in terms of the spin ($\mathbf{S}_k$) and orbital ($L_{k\mathrm{N}}^{\alpha}$) angular momentum of the (kth) electron, Equations (10) to (14):

$$\begin{aligned}\mathbf{J}_{\alpha\beta}^{(1a)} = {} & (2m/h)\mu_{\mathrm{B}}^2(\mu_0/4\pi)^2\gamma_{\mathrm{N}}\gamma_{\mathrm{N}'}\langle 0|\sum_k r_{k\mathrm{N}}^{-3}r_{k\mathrm{N}'}^{-3} \\ & [(\boldsymbol{r}_{k\mathrm{N}}\cdot\boldsymbol{r}_{k\mathrm{N}'})\delta_{\alpha\beta} - r_{k\mathrm{N}}^{\alpha}r_{k\mathrm{N}'}^{\beta}]|0\rangle \qquad (10)\end{aligned}$$

$$\begin{aligned}\mathbf{J}_{\alpha\beta}^{(1b)} = {} & (1/h)(2\mu_{\mathrm{B}})^2(\mu_0/4\pi)^2\gamma_{\mathrm{N}}\gamma_{\mathrm{N}'}\sum_n({}^1E_n - E_0)^{-1} \\ & \times\left\{\langle 0|\sum_k r_{k\mathrm{N}}^{-3}L_{k\mathrm{N}}^{\alpha}|n\rangle\right. \\ & \left.\times\langle n|\sum_j r_{j\mathrm{N}'}^{-3}L_{j\mathrm{N}'}^{\beta}|0\rangle + \mathrm{cc}\right\} \qquad (11)\end{aligned}$$

$$\begin{aligned}\mathbf{J}_{\alpha\beta}^{(2)} = {} & (-1/h)(2\mu_{\mathrm{B}}\hbar)^2(\mu_0/4\pi)^2\gamma_{\mathrm{N}}\gamma_{\mathrm{N}'}\sum_n({}^3E_n - E_0)^{-1} \\ & \times\left\{\langle 0|\sum_k 3r_{k\mathrm{N}}^{-5}(\mathbf{S}_k\cdot\mathbf{r}_{k\mathrm{N}})r^{\alpha}{}_{k\mathrm{N}} - r_{k\mathrm{N}}^{-3}\mathbf{S}_k^{\alpha}|n\rangle\right. \\ & \left.\times\langle n|\sum_j 3r_{j\mathrm{N}'}^{-5}(\mathbf{S}_k\cdot\mathbf{r}_{j\mathrm{N}'})r_{j\mathrm{N}'}^{\beta} - r_{j\mathrm{N}'}^{-3}\mathbf{S}_j^{\beta}|0\rangle + \mathrm{cc}\right\} \qquad (12)\end{aligned}$$

$$\begin{aligned}\mathbf{J}_{\alpha\beta}^{(3)} = {} & (-1/h)(16\pi\mu_{\mathrm{B}}\hbar/3)^2(\mu_0/4\pi)^2\gamma_{\mathrm{N}}\gamma_{\mathrm{N}'} \\ & \times\sum_n({}^3\mathrm{E}_n - \mathrm{E}_0)^{-1}\left\{\langle 0|\sum_k\delta(r_{k\mathrm{N}})\mathbf{S}_k^{\alpha}|n\rangle\right. \\ & \left.\times\langle n|\sum_j\delta(r_{j\mathrm{N}'})\mathbf{S}_j^{\beta}|0\rangle + \mathrm{cc}\right\} \qquad (13)\end{aligned}$$

For references see page •••

$$\mathbf{J}^{(4)}_{\alpha\beta} = (-2/h)(16\pi\mu_B\hbar/3)(2\mu_B\hbar)(\mu_0/4\pi)^2\gamma_N\gamma_{N'} \times \sum_n ({}^3E_n - E_0)^{-1} \left\{ \langle 0| \sum_k \delta(r_{kN})\mathbf{S}^\alpha_k |n\rangle \times \langle n| \sum_j 3r^{-5}_{jN'}(\mathbf{S}_k \cdot \mathbf{r}_{jN'})r^\beta_{jN'} - r^{-3}_{jN'}\mathbf{S}^\beta_j |0\rangle + \text{cc} \right\} \quad (14)$$

where cc indicates the conjugate term in which the two operators are switched. μ_B is the Bohr magneton, γ_N is the magnetogyric ratio for the nucleus N. $\delta(r_{kN})$ is the Dirac delta function which picks out the value at $r_{kN} = 0$ in any integration over the coordinates of the kth electron.

The coupling contributions $\mathbf{J}^{(1a)}$ or $\mathbf{J}^{(OD)}$ and $\mathbf{J}^{(1b)}$ or $\mathbf{J}^{(OP)}$ can be thought of as arising through paramagnetic and diamagnetic currents induced in the molecular electronic distribution by the nuclear magnetic moment of one of the nuclei, coupling to the magnetic moment of the other nucleus. The coupling contribution $\mathbf{J}^{(3)}$ or $\mathbf{J}^{(FC)}$ can be considered as arising from the transmission of spin information from nuclear spin to electron spin due to the finite density of the electron at the nucleus, this information is passed on through the spin interaction between electrons in the molecule and transmitted at the other end via electron spin density at the other nucleus. The dipole–dipole interaction between the nuclear and electron spins lead to the coupling contribution $\mathbf{J}^{(2)}$ or $\mathbf{J}^{(SD)}$.

The expressions shown here in Equations (9)–(14) are cast in the form of sums over excited states, as they were originally cast in the Ramsey formulation. However, practical calculations are not actually carried out in this form for several reasons. Multiple perturbation theory is more conveniently carried out by using directly the first order perturbed wavefunction or the first order density matrix. In other words, for the multiple perturbation of the external magnetic field and the nuclear magnetic moment, the nuclear magnetic shielding may be calculated by first calculating the first order density matrix of the molecule in the external magnetic field alone, using the operator $\sum_j L^\beta_{j0}$, and with this the integrals that account for the second perturbation imposed by the nuclear magnetic moment are then evaluated, using the operator $\sum_k r_{kN}{}^{-3}L^\alpha_{kN}$. Or independently, one could first find the first order density matrix of the molecule in the presence of the nuclear magnetic moment alone, and with this, the integrals that account for the second perturbation imposed by the external magnetic field are evaluated. A physical interpretation is that the nuclear magnetic shielding arises from the interaction of the magnetic moment of the nucleus with the magnetic field due to the current density induced by the external magnet or, equivalently, from the interaction of the current density induced by the nuclear magnetic moment with the external magnetic field. The most common approach is to construct first the electronic response induced by the external magnet and then study its interaction with various nuclei in the molecule. Note that written in the form of Equation (9), the diamagnetic part of the shielding is very easy to calculate, since it requires an average over the unperturbed electronic ground state function only. On the other hand, the second order term, the paramagnetic contribution, requires a knowledge of how the presence of the external magnetic field changes the electronic wavefunction of the molecule and the integration requires that this knowledge be especially accurate in the immediate vicinity of the nucleus of interest.

The calculation of the electric field gradient tensor does not require a perturbation treatment since this is one of those electronic properties that can be calculated as an average over the electronic ground state wavefunction. The zz component of the electric field gradient tensor is given by Equation (15)

$$q_{zz} = \sum_j e_j(3z_j^2 - r_j^2)r_j^{-5} \quad (15)$$

where e_j is the charge of the jth particle (the electrons, other nuclei, external charges) in the system and the z axis is in the nuclear-fixed coordinate system, that is along the nuclear axis of spin. The spin axis of the nucleus is allowed to rotate with respect to the laboratory frame of reference and the nuclear wavefunction will be a product of the intrinsic $\Psi_{\text{intrinsic}}$ and orientation $\Psi_{I,M}$ functions for spin angular momentum described by quantum numbers I and M, Equation (16)

$$\Psi_{\text{total}} = \Psi_{I,M} \cdot \Psi_{\text{intrinsic}} \cdot \Phi(\text{electrons, other nuclei, external charges}) \quad (16)$$

For a nucleus in a molecule oriented in the laboratory framework, the components of the field gradient tensor are q_{XX}, q_{YY}, q_{ZZ}. The principal field gradient tensor component q_{zz} is related to the laboratory values through the direction cosines between the axes, as follows, Equation (17):

$$q_{zz} = (C_{Xz})^2 \cdot q_{XX} + (C_{Yz})^2 \cdot q_{YY} + (C_{Zz})^2 \cdot q_{ZZ} \quad (17)$$

In the absence of a magnetic field, the energy of a quadrupolar nucleus in the electric field gradient will be obtained by averaging the electric quadrupole charge over the wavefunction $\Psi_{\text{intrinsic}}$, averaging the squares of the direction cosines over $\Psi_{I,M}$, and averaging $q_{ZZ} = \sum_j e_j(3Z_j^2 - r_j^2)r_j^{-5}$ over the wavefunction Φ (electrons, other nuclei, external charges) expressed in the laboratory frame. The average of the direction cosines over $\Psi_{I,M}$ leads to an energy expression that is proportional to $[3M^2 - I(I+1)]$ in the absence of a magnetic field.

In the presence of a magnetic field, the magnetic dipole moment of a quadrupolar nucleus, which lies along the axis of symmetry of the cigar-like or pancake-like nuclear charge distribution, interacts with the magnetic field. Thus, when a single quadrupolar nucleus in a molecule is placed in a magnetic field, the interaction of the electric quadrupole with the internal electric field gradient at the nuclear site in the molecule leads to a series of $2I$ resonance lines. Thus, a spin $I = 1$ nucleus in an axially symmetric electric field gradient gives a pair of lines separated by $[e^2 q_{ZZ} Q](3/2)$ or more explicitly, by $[e^2 q_{zz} Q](3/2) \cdot (3\cos^2\theta - 1)/2$, where θ is the angle that the principal symmetry axis of the electric field gradient makes with the external magnetic field. The pair of lines is centered at a frequency that provides the shielding tensor. Both the shielding tensor and the electric field gradient tensor in the XYZ (i.e. the laboratory-fixed) coordinate system can be obtained from an oriented molecule in the solid state. Equation (17) permits the determination of the tensor in the xyz (i.e. the molecule-fixed) coordinate frame system. Since the electric field gradient is a traceless tensor, the isotropic average is zero. Thus, in the liquid phase the positions of the lines in the NMR spectrum are not affected by the nuclear quadrupole coupling, although information about the latter can still be obtained from quadrupolar relaxation times.

Theoretical calculations of the electric field gradient tensor in *the molecular frame* of an isolated molecule involves evaluating the quantum mechanical average of the operator $q_{zz} = \sum_j e_j(3z_j^2 - r_j^2)r_j^{-5}$ over the ground state electronic wavefunction for the molecule, where j runs over all electrons and the origin is set at the nucleus in question. To this electronic contribution must be added the nuclear contribution, by evaluating a similar algebraic expression in which e_j are the charges of the other nuclei and z_j and r_j are their positions in the molecular framework with the origin at the nucleus in question. For molecules in a liquid, electric field gradient contributions from neighbors have to be included, which may require a quantum mechanical average or an approximate sum over fixed partial charges.

2.2 Gauge Origin Problem in Calculations of Chemical Shift

In deriving the expressions shown here, the external magnetic field **B** itself does not appear in the Hamiltonian. What appears instead are the magnetic vector potentials associated with the magnetic fields, Equation (18):

$$\mathbf{B} = \nabla \times \mathbf{A} \tag{18}$$

where ∇ is the gradient vector. That is, $B_z = (\partial A_y/\partial x) - (\partial A_x/\partial y)$, for one component. While **B** is determined uniquely if **A** is given, unfortunately, there is an ambiguity because there is no unique **A** that produces a given **B**. Any transformation that takes a particular **A** into another functional form that also reproduces the same **B** upon applying Equation (18) is called a gauge transformation. A mere translation of the origin of the coordinate system can do this, therefore the set of problems associated with this ambiguity is called the gauge origin problem. Physically, there should be no problem at all, since an arbitrary choice of coordinate system should not affect an observable property. Similarly, theoretically there should be no problem at all, any physical quantities resulting from any calculations involving **A** or **B** or physical quantities related to them must be gauge invariant, provided the calculations are done exactly. In fact, calculations are not usually done exactly when one uses an incomplete set of basis functions in which to do the calculations. It has been shown that if the Hartree–Fock equations are solved exactly (which is only possible in the limit of a complete basis) the total current density is gauge independent, as is the nuclear magnetic shielding σ, while the two parts which are usually called the "diamagnetic" and "paramagnetic" contributions in Equation (18) are not individually gauge invariant. In practice, calculations are not carried out in the Hartree–Fock limit so the results of such calculations are not gauge invariant. When a single origin is chosen common to all electrons in the molecule in the definition of $\sum_j L_{j0}^{\beta}$ (and r_{j0}), the method is the so-called "common origin" coupled Hartree–Fock (CHF) method.

Consider an isolated atom. The external magnetic field induces a current density. The current density vector is orthogonal to the magnetic field vector **B** and to the position vector r_j. For a magnetic field in the z direction the current density vectors lie in planes parallel to the xy plane, following the tangents of concentric circles. Here, the natural choice of origin is the position of the nucleus; this leads to a vanishing paramagnetic current density. The current density is entirely the diamagnetic part and corresponds to a local field that opposes the external field **B**. Moving the origin off-center to other than the position of the nucleus would make the two parts more difficult to evaluate, but the sum should still be the same as before, so there is no reason to adopt an alternative origin. In molecules, however, there is no choice of origin that will make the paramagnetic part vanish. Changing the location of the origin, in the definition of r_{j0} and $\sum_j L_{j0}^{\beta}$ in Equation (18) leads to differing amounts of positive and negative terms. The worst choice gives very large not quite canceling terms. Clearly, the inner shell electrons in a molecule behave like they do in the free atom, so that it makes sense to choose the nucleus as the origin when calculating integrals over orbitals centered on that atom. However, that same origin would be a bad choice for orbitals centered on another atom, whereas choosing the

For references see page •••

nucleus of that atom as origin would present a favorable atom-like calculation for its own inner electrons. Thus, it becomes clear that in order to avoid calculating large positive and negative terms which imperfectly cancel in a single origin method, some method of using distributed origins would present a practical advantage in computing nuclear magnetic shielding for nuclei in molecules.

The theoretical calculations of nuclear magnetic shielding did not become generally practical even for very small molecules until (1) various ways of using distributed origins were devised, and (2) efficient algorithms for evaluating second order properties were developed. The various schemes for using distributed origins are known by the acronyms LORG (localized orbital/local origin),[6] IGLO (individual gauge for localized orbitals),[7] GIAO (gauge including atomic orbitals),[8] and IGAIM (individual gauges for atoms in molecules).[9] The success of distributed origins comes from the avoidance of calculating large imperfectly canceling contributions. In the first two methods, gauge factors are applied to localized molecular orbitals instead of every atomic orbital. The LORG and IGLO methods introduce an approximation in the form of the closure relation and LORG uses commutation rules and identities. Both have been very successful, although there is the problem of lack of uniqueness in the localization method used. The GIAO method uses gauge factors on every atomic orbital. Although this method of distributed origins had been introduced much earlier than all the others, it was not until the efficient implementation by Peter Pulay using the analytic gradients approach that it became widely successful. The convergence of calculated σ values with increasing quality of basis set employed appears to be faster with the GIAO method. GIAOs (sometimes called London orbitals) constitute a physically motivated, compact basis set for magnetic calculations. The field dependent exponential factor in the London orbital depends on the origin of the coordinate system. A displacement of the origin changes the phase factor of an orbital centered on a nucleus by a factor which is independent of the electronic coordinates. Thus, the calculated properties such as shielding remain unaffected and methods based on the use of such orbitals are gauge invariant. The most important property of the GIAO method is not this formal translational invariance but that the GIAO (the atomic orbital multiplied by the gauge factor) itself represents to first order the eigenfunctions of a one-electron system which has been perturbed by an external magnetic field. GIAOs thus incorporate the bulk of the effect of the magnetic field at the basis function level. The IGAIM approach amounts to constructing the induced current density distribution of a molecule from its constituent atoms, following the highly successful atoms in-molecules concepts of R.F.W. Bader. It differs from LORG, IGLO, and GIAO in that the gauge origins are determined by properties of the charge density in real space rather than by the behavior exhibited by the basis functions in the Hilbert space of the molecular wavefunction. All these distributed origin methods (GIAO, IGLO, LORG, IGAIM) and any single common origin method should lead to identical results at the Hartree–Fock level in the limit of a complete set of basis functions. The differences lie in the rate of convergence as the number of basis functions are increased. The various distributed origins methods converge toward the Hartree–Fock limit faster than using a single origin. Common origin calculations require much larger basis sets to provide nearly origin-independent results comparable to the results from distributed origin methods. An alternative method of doing calculations with a single origin is to cast the diamagnetic term in the same (a SOS) form as the paramagnetic term.[10] This makes the rate of convergence of the calculations of the two parts equally slow and the calculations equally difficult. This (Geertsen's method) has the virtue of being origin-independent (i.e. gives the same answer for any choice of common origin) at any basis set size.

2.3 Difficulties of Describing Triplet States in Calculations of Spin–Spin Coupling

There are no gauge problems in spin–spin coupling calculations; as seen in Equations (10)–(14) only operators with their origin at the nucleus (r_{kN} and $r_{kN}^{-3}L_{kN}^{\alpha}$) appear. The calculations of spin–spin coupling have their own associated difficulties. As can be seen in Equations (10)–(14), the nature of some of the indirect spin–spin coupling mechanisms requires calculations with uncoupled spin states. Thus, the spin unrestricted approaches that are normally applied to open shell systems have to be used. When there is a nonsinglet ground state with lower energy than the restricted Hartree–Fock singlet ground state, the calculations of the $\mathbf{J}^{(SD)}$ and $\mathbf{J}^{(FC)}$ terms require higher order calculations than CHF. Furthermore, the usually (not always) dominant FC contribution in Equation (13) requires that the spin densities are highly accurate at the location of the nucleus, and this is not easily achieved when the basis functions used are the standard gaussian form, having no cusp at the nucleus. Relativistic effects influence spin–spin couplings much earlier (at lower atomic numbers) than other properties due to the strong dependence of $\mathbf{J}$ on the electronic structure at the position of the nucleus and its immediate vicinity. In fact, the Equations (10)–(14) are valid only for the point nucleus in the nonrelativistic limit. For heavy nuclei it is necessary to start out with the relativistic treatment described in section 2.6, since the nonrelativistic theory may lead to unrealistic calculated values.[11]

2.4 Ab Initio Methods

In ab initio calculations of NMR parameters there are several things that have to be considered: (1) the level of theory that is used (without, with some, or with substantial electron correlation, with or without relativistic corrections), (2) the number of basis functions, (3) the desired degree of averaging over molecular configurations (with or without rovibrational averaging, with or without medium effects), (4) the availability of tensor data, and (5) the availability of absolute shielding test data in the case of chemical shifts. In the case of spin–spin coupling, there is very limited information beyond that of the isotropic average values obtained in solution. Only in extremely rare cases is there anisotropy information, so that the only viable additional tests are those of isotopic effects on spin–spin coupling. In the case of ^{13}C chemical shifts the amount of detailed tensor information from single crystals and polycrystalline powders is so rich that the level of theory, and size of basis sets needed, and the accuracy of geometrical structure data required to achieve agreement with experiment has been established (by D.M. Grant and associates) for a large variety of carbon site types. The level of theory used in ab initio calculations of NMR parameters had to improve continuously with the challenges posed by attempts to match experimental results for specific small molecules, as we shall see below (section 3.1). Depending on the need for accuracy, depending on the nucleus and the nature of the nuclear site, the appropriate level of calculation can be done. Various levels of theory have been used with various numbers of basis functions. The need to establish good basis functions still hinders accurate calculations for transition metal nuclei. Furthermore, in some cases there is a lack of a good test molecule in the gas phase for which absolute shielding has been established. For the purpose of distinguishing between two structures or even two chemical identities, calculations of σ using uncorrelated wavefunctions constructed with smallish basis sets have sometimes been employed. This is a very dangerous approach, which has been criticized. Ideally, a calculation to estimate the importance of electron correlation to the nuclear shielding should be done. An estimate of the magnitude of the effects of averaging over molecular configurations is needed, in order to determine whether it is sufficient to do a calculation for a single molecule at a fixed geometry in a vacuum. An estimate of the magnitude of relativistic effects on shielding is needed when next neighbors are halogen atoms, or when the nucleus is a heavy nucleus. The involvement of multiple bonds or presence of lone pairs at the nucleus of interest is usually an indication that correlated methods have to be used.

An alternative to the CHF approach is the use of polarization propagator or the equation of motion (EOM) methods. With these latter two methods the level of calculation equivalent to the CHF level is the random phase approximation (RPA). For the same basis set, using the same origin choice, calculations using CHF and RPA should provide the same results. In terms of perturbation theory, the RPA is the consistent first order approximation to the polarization propagator or the EOM. The CHF, RPA, and the first order polarization propagator method represent *the same approximation* for frequency independent properties such as the NMR properties σ and **J**. With respect to the extent of inclusion of electron correlation, CHF and RPA provide the first level of calculations.

In the finite field method, the NMR parameter (for example, **J**) is obtained by differentiating the energy in the presence of the nuclear magnetic moments (or in the presence of the nuclear moment and the external magnetic field for σ) with respect to the nuclear moments (or with respect to the nuclear moment and the external field, for σ). The addition of a finite field to the total energy expression is a simple extension of existing computer codes for electronic structure calculations and is one of the standard methods for calculating higher order molecular electronic properties such as the nonlinear polarizabilities, for example. Thus, the finite field method is easily used, without additional theoretical development, to study the effects of electron correlation on properties. The drawback is that a finite field calculation has to be carried out for each tensor component of the property. Thus, while the purely isotropic FC term of **J** is easily done with finite field methods at various levels such as various many body perturbation theory (nth order term) (MBPT(n)) and various coupled cluster (CC) methods, the tensor types of mechanisms given in Equations (10) to (12) and (14) require several calculations to yield the various xx, xy, xz, yy, zz, components. Direct methods such as the polarization propagator or EOM method on the other hand, use analytic expressions that provide all components of the tensor with one calculation. In an MBPT(n) calculation, or alternatively the Møller–Plesset nth order term (MPn) perturbation series, all energy contributions less than or equal to order n in perturbation theory are included. CC methods on the other hand, in addition to being consistent to a particular order in perturbation theory include certain classes of energy contributions summed to infinite order. The same kind of infinite summations are also included in polarization propagator methods (RPA, SOPPA, etc.). Thus, SOPPA (Second-order polarization propagator approximation) is not equivalent to the MBPT(2) (Second order many body perturbation theory) or MP2 (Møller–Plesset second order term) level of approximation. The coupled cluster

For references see page •••

reference state including singles and doubles excitations (CCSD) has been introduced in post Hartree–Fock shielding calculations by Gauss, CC has been used in finite field calculations of $\mathbf{J}^{(FC)}$ by Bartlett et al. and has been used in the polarization propagator method as an extension of SOPPA for the calculations of all the mechanisms of **J**.

For chemical shift calculations the CHF level, sometimes also referred to as the self consistent field (SCF) level since the calculations use the SCF wavefunctions, appears to give quite good results for CH_4 and other saturated ^{13}C sites, and even olefinic sites. The major problems that have been discovered for carbon are the C≡O, –C≡N, and >C=O environments, for which sites electron correlation is extremely important. The SCF level has been found to be insufficient even for calculations using very large basis sets to reproduce the anisotropy of the ^{31}P shielding in the molecule PH_3.[12] Apparently, electron correlation is important for ^{31}P calculations in molecules where a lone pair is on the phosphorus, even when only hydrogen atoms are attached to it. In these cases, some level of post-Hartree–Fock theory is necessary in order to obtain meaningful results.

The next level of theory for shielding provides electron correlation effects at the level of MBPT(2) or MP2 perturbation theory. MP2 calculations may be carried out with a conventional common origin or may be used with any of the distributed origin approaches. An alternative approach to second order electron correlation effects called SOPPA belongs to the family of propagator techniques, but is different from and not equivalent to MP2. Many quantum mechanical software packages provide MP2 level of wavefunctions. These are supposed to take care of the dynamic correlation effects and hence to improve results for closed shell systems where CHF already gives good results. When the degree of electron correlation contribution to the shielding is small, this level is usually sufficient to provide useful comparisons with experiment. When the difference between SCF and MP2 results is not small, then it may be necessary to go up to MP4 level, with the corrections at MP2, MP3, and MP4 often alternating in sign. Despite its successes, the inherent problem with this approach is the slow convergence of the perturbation series for those systems with strong correlation effects, that is for those cases where MBPT(2) or MP2 level is no longer adequate.

Multiconfiguration self consistent field wavefunctions (MCSCF) may sometimes be necessary for calculations of shielding, when the electronic ground state cannot be adequately described by a single Slater determinant. A multireference calculation can properly account for strong correlation effects if closed shell SCF is too poor as an initial approximation (for example, in O_3, NSF, SO_2, N_2O_3 molecules). CHF methods completely fail for such systems. MCSCF wavefunctions, generated using complete active spaces (CAS) and restricted active spaces (RAS), may be used with any of the distributed origin methods, spawning such methods as MCSCF/GIAO[13] and MCIGLO (multiconfiguration individual guage for localized orbitals)[14]. The MCIGLO formulation was presented formally by van Wüllen and Kutzelnigg,[14] and applied to appropriate cases such as carbenes and dinitrogen oxides.[14] The dinitrogen oxides $(NO)_2$, $(NO)(NO_2)$, and $(NO_2)_2$ have strong correlation effects which affect the shielding tensors. The ^{15}N and ^{17}O shieldings have been measured in these molecules and the effects of correlation are particularly interesting in that they are of both signs. In the nitroso nitrogen, the electron correlation effect is to enhance deshielding, while in the nitro nitrogen the correlation effects are to increase shielding. Thus, in $(NO)(NO_2)$ the correlation effects are large and opposite in sign for the two types of N. Correlation contributions to the isotropic ^{15}N shielding range are −558 ppm in $(NO)_2$, +61 ppm in $(NO_2)_2$ and −63 and +116 ppm in $(NO)(NO_2)$.

If different electronic configurations dominate the wavefunction at different geometries, the calculation of the shielding surface also requires a computational method based upon a multiconfiguration wavefunction.[14] The MCSCF approaches are hampered by the same sort of problem because rather large active spaces are needed to obtain satisfactorily converged results. While static correlation effects on shielding arising from near degeneracies are efficiently treated by the MCSCF methods described above, many body perturbation theory (MBPT, also known as Møller–Plesset perturbation theory) has been used to treat dynamical correlation effects.[15–17]

One of the most successful approaches for the treatment of electron correlation is provided by CC theory. While ultimately based on a single determinant reference function, the exponential parametrization of the wavefunction ensures an efficient treatment of electron correlation. In particular, dynamic correlation effects are accounted for with nearly quantitative accuracy at a fraction of the cost needed to obtain similar precision with MCSCF approaches. Among the various schemes suggested in the literature, the CCSD approximation[18] in which single and double excitations are considered in the cluster operator, has proven specially useful in calculations of other molecular properties. CC approaches can be considered as infinite-order generalizations of the MBPT series. The implementation of GIAOs for the CCSD approach has been carried out by Gauss and Stanton,[19] and further augmented by a perturbative correction for connected triple excitations coupled cluster singles and doubles with some triple excitations (CCSD(T)).[20] The principal advantage of the GIAO method is the ease

with which high level treatments of electron correlation may be handled by straightforward application of analytic derivative theory.

MCSCF/GIAO calculations for triple-bonded systems, in particular HC≡N, HN≡C, MeC≡N, and MeN≡C[21] show that the electron correlation effects are large for the triple-bonded nuclei, especially the component perpendicular to the triple bond axis, and largest for the terminal nucleus. For example, the electron correlation contribution to $\sigma_{\perp}^{13}$C shielding is +47 to +54 ppm in the $-N\equiv{}^{13}C$ nuclear sites, and to $\sigma_{\perp}$ nitrogen shielding is +87 to +79 ppm in the −C≡N sites.[21] These MCSCF/GIAO results do not compare as well with experiments as do the calculations by Gauss using the CCSD method.[19,20] The ultimate level of theory would be full configuration interaction (FCI), but this is only possible for very small systems and is rarely used.[22]

The same general methods for multiple perturbations are used for calculating spin–spin couplings, with the difference that there are no gauge origin problems in spin–spin coupling calculations. All but the $\mathbf{J}^{(OD)} + \mathbf{J}^{(OP)}$ mechanisms mix triplet states with the unperturbed electronic singlet ground state. Thus, the unrestricted Hartree–Fock (UHF) method is sometimes used to generate the unperturbed electronic ground state, even for closed shell molecular systems such as CH_4. The extent to which electron correlation needs to be included depends on the system, just as in shielding calculations. The same molecules that are found to be pathological cases in shielding calculations also pose problems in spin–spin coupling calculations. The uncorrelated finite field SCF calculations, which are the same approximation as CHF and RPA calculations, in most cases give good results for σ while this is not often true for $\mathbf{J}$. The $\mathbf{J}^{(OD)}$ term in spin–spin coupling, like the diamagnetic part of σ is generally easy to calculate; good results can be obtained with low level electronic correlation included and using moderately sized basis sets. The sum over all excited states in $\mathbf{J}^{(OP)}$ extends over singlet excited states since most of the common ground states that chemists are interested in are singlet states. However, in the $\mathbf{J}^{(SD)}$, $\mathbf{J}^{(FC)}$ and $\mathbf{J}^{(SDFC)}$ expressions, the excited states have different spin multiplicity from the ground state. Because there is a state of triplet symmetry either very close to or sometimes below the restricted Hartree–Fock singlet ground state for many molecules, these mechanisms for spin–spin coupling are very poorly described at the CHF level of approximation. This problem affects spin–spin coupling calculations, but not calculations of σ. A resurgence of interest in accurate ab initio calculations of coupling constants was initiated by Oddershede and others[23–25] using polarization propagator methods. The SOPPA has been found to yield reliable coupling constants in some instances.[23,26] When higher accuracy is required, CCSD reference states (limited to single and double excitations) have been used within the polarization propagator method.[26,27] Midway between first (RPA) and second order is HRPA (higher random phase approximation), which has been used by Galasso in the EOM approach to calculate one- and two-bond coupling constants $^{1\text{ or }2}\mathbf{J}$(CC) in ring systems.[28] MCSCF wavefunctions are appropriate in cases where the SCF calculations predict unrealistic coupling constants,[29–31] such as in (pathological) molecules involving multiply bonded nitrogens.[30] The method is MCLR (multiconfiguration linear response).[29] MCSCF functions have been used for the hydrides of group IV (C, Si, Ge, Sn).[31] Finite field methods have been used by Bartlett et al. to calculate the FC mechanism of spin–spin coupling using various levels including electron correlation, up to CCSD.[32] MBPT has also been used.[33]

2.5 Density Functional Methods

One method of including electron correlation effects is through density functional theory (DFT). DFT methods have become widely used. DFT methods are based on a theorem which states that for a scalar potential $V(\mathbf{r})$ the ground state N-electron density uniquely determines the potential that gives rise to it. The total electronic energy is a unique functional of the density $\rho(\mathbf{r})$.[34] Although constructing an accurate approximation to the kinetic exchange correlation functional $G[\rho(\mathbf{r})]$ is a formidable task, it need only be done once because the form of G is independent of the form of $V(\mathbf{r})$. Approximations are required because the functional is not known exactly but these approximations are getting better and better. Developments in exchange correlation functionals have made DFT methods viable alternatives to those of conventional quantum mechanical calculations. DFT combines the promise of accurate results (that is, more accurate than Hartree–Fock level quantum calculations) with cheaper computation (because it scales up to more electrons less steeply than conventional methods that include some electron correlation). Several approximate functionals of the electron density are in common use and are relatively successful in prediction of molecular structure, and are known to yield geometries and energies of at least MP2 quality. The difficulties of calculating magnetic response properties using DFT arise in two major ways. The first is intrinsic to all DFT methods, because only approximate functionals are available and they are deficient in various ways. NMR parameters show up these deficiencies most glaringly because of their extreme sensitivity to the electron distribution in the immediate vicinity of the nucleus. Second, is that in the presence of a vector potential (when magnetic fields or magnetic moments are present) the functionals of both

For references see page •••

the current density and the electron density are needed, thus a current density functional theory (CDFT) is the appropriate theory. A current-dependent DFT has been derived by Vignale et al.[35–37] Handy et al. have used this approach.[38] On the other hand, more commonly, a generalization of the Kohn–Sham density functional theory (KSDFT) has been used to obtain magnetic responses using only the functional of the electron density; the current density part of the calculation is not included. This is by far the most commonly used calculation method. It remained to be shown by Grayce and Harris[39,40] that when the magnetic field is produced by a constant applied field and a single nuclear magnetic dipole, the current density is a functional of the electron density. Furthermore, they showed that in the linear response regime, the current density functional depends on the *zero field electron density*. As a consequence, magnetic responses in the linear regime are solely functionals of the electron density in the absence of a magnetic field. Grayce Harris call this the magnetic field density functional theory (BDFT).[39,40] The problem is that in all DFT approaches, only *approximate* functionals are yet available, and the magnetic response DFT approaches, whether CDFT or KSDFT or BDFT, all suffer from this same difficulty.

There are several independent formulations of DFT of shielding. A large number of DFT calculations have been carried out by Malkin, Salahub et al. without including the effects of the current density, using a local density approximation (LDA) in a SOS method and IGLO method of local origins for shielding tensor calculations.[41,42]

In the CDFT of Vignale et al., in addition to the usual exchange correlation functionals of the density that are used for solving electronic structure problems in the absence of a magnetic field, the effects of a current density are included.[35–37] Van Wüllen has derived the coupled perturbation equations for calculating nuclear magnetic shielding tensors using CDFT in both the IGLO and the GIAO method of introducing local gauge origins.[43] Lee, Handy and Colwell derived equations within the Kohn–Sham formulation of DFT for calculations of nuclear magnetic shielding tensors with GIAO basis functions using CDFT, including the use of a local exchange correlation functional which depends on both the electron density and the paramagnetic current density.[38] To put the various DFT formalisms and calculations in context they applied their working expressions to the systems HF, N_2, CO, F_2 and H_2O. By doing computations using conventional atomic basis functions versus GIAOs basis functions, using various local functionals of the density in popular use, such as the exchange functional of Becke with the correlation functional of Lee–Yang–Parr (BLYP) and others, with and without including the current-dependent functional proposed by Vignale, Rasolt and Geldart,[37] with or without the ad hoc correction of Malkin et al.[41] Lee et al.[38] provide some very useful comparisons. They of course found what is already well known, that using GIAOs leads to better results than using conventional (gaugeless) atomic basis functions employing CHF or any DFT method. They found that including the current-dependent functional proposed by Vignale, Rasolt and Geldart[37] gives only small corrections. They also established that DFT and CDFT methods exhibit general difficulty in describing multiply bonded systems such as N_2 and CO. An important observation is that calculations using local functionals of the density give severely deficient eigenvalues. To overcome this, a more accurate functional must be developed. Since the Malkin correction is to modify the energy denominators, this has the effect of shifting the incorrect eigenvalues already noted above. Indeed, direct comparisons by Lee et al. using various functionals with and without the ad hoc Malkin correction lead to a significant improvement in the CO case. They also found that, unlike in the HF molecule, exchange terms are significant in the CO molecule and the current-density terms are no longer negligibly small. The general conclusions are that the use of local density functionals is a major deficiency and overwhelms the small current density corrections.[38] The best results for CO in the Lee et al. formulation of CDFT/GIAO appear to come from the hybrid B3LYP functional[44,45] combined with the Malkin correction.[41] Thus, in spite of what appears to be a lack of solid theoretical foundation, the ad hoc Malkin correction gives very promising results.

There are several other implementations of DFT in shielding calculations, all of which use only current-independent exchange correlation functionals: the IGLO-based DFT of Malkin and Salahub already mentioned and the GIAO-based DFT calculations introduced by Schreckenbach and Ziegler,[46,47] Pulay et al.[48] and Cheeseman, Trucks, Keith and Frisch.[49]

In practice, the calculations in the Ziegler DFT/GIAO implementation employ Slater-type orbitals as atomic basis functions (unlike most computations which use Gaussian-type basis functions).[46,47] They have also used the frozen core approximation in some systems.[50] Pulay et al. have developed a DFT/GIAO based on their program system which uses analytic derivative theory (TX90).[48] They derive their DFT/GIAO equations in the density matrix formulation used originally.[8] Compared to the Hartree–Fock case, the only new quantity is the first-order exchange correlation term. In the Pulay implementation, these terms are evaluated by the same Becke numerical integration scheme they use for the exchange matrix elements themselves. Although in principle this method is identical to that of Schreckenbach and Ziegler, there are major differences in implementation. First they

use Gaussian basis functions rather than Slater basis functions. Second, the Pulay implementation does not use fitting functions for the Coulomb and exchange functions. Rather they calculate the Coulomb term exactly, using traditional two-electron integral evaluation, and calculate exchange correlation terms by the numerical integration technique of Becke. Independently, Cheeseman, et al. presented their formulation of the DFT/GIAO method and also DFT/CSGT (Continuous set of gauge transformations) (or IGAIM).[49] The latter makes use of the highly successful IGAIM[9] and the more general CSGT[51] method of Keith and Bader (wherein the current is determined through the definition of a CSGT, a separate gauge origin to calculate the current $\mathbf{J}^{(1)}(\boldsymbol{r})$ at each point $\boldsymbol{r}$ in real space). They found the IGAIM results essentially identical to the CSGT. Cheeseman et al. compared the results from the DFT methods with CHF/GIAO and CHF/CSGT calculations of isotropic nuclear magnetic shielding of ^{13}C in a large number of molecules.[49]

How well does DFT predict absolute shielding? DFT accounts for correlation effects implicitly in the exchange correlation functionals used and thus might be expected to give superior results in comparison to CHF calculations for a given GIAO set of basis functions, in those molecules such as CO, N_2, NNO, HCN where electron correlation effects on shielding are important. Absolute shieldings obtained using the gradient-corrected functionals are consistently better than CHF in these molecules,[49] although the improvement is small in some cases. Using a basis set which is sufficient to predict accurate shifts using GIAO/MP2 theory, various DFT functionals consistently predict chemical shifts that are too deshielded compared with experiment. The absolute shielding results are too deshielded by 10–20 ppm for ^{13}C, by 6–40 ppm for ^{15}N, and by 30–40 ppm for ^{17}O in the selected molecules where the absolute shielding results were known. Anisotropies are even worse. The isotropic chemical *shifts* correlate better with experiment, with somewhat smaller average standard deviation in the DFT results in comparison with experiment compared to CHF using GIAOs. The test of any theoretical method for calculating σ is the comparison of the results with the benchmark CCSD(T) calculations of Gauss for a set of small molecules at the same fixed geometries. The successful wide applicability of the DFT method for calculating σ lies in its applications to molecules with large numbers of electrons, where the accurate CCSD(T) calculations are not feasible and even MP2 level calculations are prohibitively expensive and impractical.

The DFT method has severe limitations for the calculations of spin–spin coupling which are connected to the inability of the presently available exchange correlation functionals (LDA and general gradient approximation) to produce the highly accurate spin densities required to describe properly the FC term for molecules containing atoms lying at the right of the periodic table and containing lone pairs.[52] The $\mathbf{J}^{(OD)}$ term is the easiest to calculate, a straightforward numerical integration in the DFT method because this contribution depends only on the unperturbed ground state density. The calculations of the $\mathbf{J}^{(OP)}$ and $\mathbf{J}^{(FC)}$ terms, just as in the ab initio calculations of $\mathbf{J}$, require the spin-unrestricted approach which is normally applied to open shell systems. The $\mathbf{J}^{(SD)}$ contribution is the most time-consuming and is usually neglected in DFT calculations of $\mathbf{J}$ because it is usually smaller than the error in the $\mathbf{J}^{(FC)}$ calculation by this method. Improved results will require a better exchange correlation functional to describe the spin polarization more precisely. A parameterized functional trained to reproduce a set of gas phase isotropic hyperfine coupling constants in nonsinglet radicals would be a good start.

2.6 Relativistic Calculations

It is well known that relativistic effects are very important in the study of heavy elements. Instead of the Schrödinger equation one has to solve a many electron generalization of the four-component Dirac equation. Fully relativistic calculations are very time-consuming even at the SCF level. Other approaches are based on perturbation theory, starting from a nonrelativistic calculation as zeroth order approximation. A direct perturbation theory formalism has been proposed by Kutzelnigg in 1990 and recently he and his co-workers have laid out the formalism for stationary direct perturbation theory which is conceptually strictly equivalent to a theory in terms of four-component spinors, but operationally on a two-component or even one-component level, and yet avoiding the singularities that arise in using other approaches.[53] The formulation is a relativistic Hartree–Fock theory for closed shell states describable by a single Slater determinant. The eagerly awaited next step is yet in progress, application of multiple perturbation theory formalism to treat relativistic effects on molecular properties such as shielding. Meanwhile, present relativistic calculations of nuclear magnetic shielding are still very approximate.

The relativistic effects on shielding may be considered in three parts. One is the direct effect of the relativistic contraction of s and p inner shells and the relativistic SCF expansion of d and f shells on the diamagnetic contribution. The contraction of the s and p shells leads to larger values of $\langle r_{kN}^{-3} \rangle$ and $\langle r_{kN}^{-1} \rangle$. The essentially constant relativistic effect on the diamagnetic contribution coming from the core electrons can be a large correction but hardly changes as the atom is compared from one molecule to the next. This is of little concern in taking differences, the chemical shifts. Another relativistic

For references see page •••

effect is the indirect effect of this s and p contraction and d and f expansion within the Hartree–Fock scheme, an effect that varies from one molecule to the next. Both of these relativistic effects are "spin-free" in nature. Third is the effect of introducing the spin–orbit terms. To calculate the additional contributions to the nuclear magnetic shielding associated with spin–orbit interactions, the latter has been approached approximately by a nonrelativistic treatment with the spin–orbit operator added on as a perturbation. These corrections can be large for nuclei whose immediate neighbors are atoms that have large values of spin–orbit coupling constants, e.g. the heavier halogens. Both the spin-free relativistic term and the spin–orbit terms can be important and they can couple with each other, as they do in ^{199}Hg shielding in mercury halides.[54] One way of approximately including relativistic effects is to use relativistic effective core potentials. Nakatsuji et al. have introduced this and other additional approximations.[55] The so-called normal halogen dependence of chemical shifts (increasing shielding upon substitution of neighboring atoms by Cl, Br, I, in that order) which had previously been attributed to relativistic effects,[56] has been accounted for entirely by the spin–orbit contributions centered on the halogen atoms in approximate calculations of shielding of ^{1}H, ^{13}C, ^{29}Si, ^{71}Ga, and ^{115}In nuclei in the respective halides.[55,57,58]

These approximate calculations have established the importance of the spin–orbit terms for shielding of nuclei having Cl, Br and I neighbors. However, calculations of heavy atom shielding are not yet on a sound footing at the level of relativistic theory used here. Furthermore, the number of electrons involved is very large and basis sets used are far from saturated so that it is not yet possible to have good nonrelativistic baseline values against which it may be possible to judge quantitatively that the relativistic approximations used are bridging the gap between nonrelativistic calculations and experiment. When a robust method is used which is consistent in the level of inverse powers of the speed of light used for each term, as is promised by the Kutzelnigg approach,[53,59] for example, coupled with a serious basis set study, this problem will be more rigorously addressed. The second problem which is just as important is the lack of experimental absolute shielding data in the gas phase for such heavy nuclei. This leads to comparisons of theoretical values with solution data where solvent effects may even bring some doubt as to the actual chemical species being observed. The problem is particularly severe with the calculations involving bare anions of In, for example, rather than neutral species.

The spin–spin coupling is itself a purely relativistic phenomenon. However, starting from a relativistic Hamiltonian such as the Dirac–Coulomb–Breit Hamiltonian, and neglecting the small components of the four component functions, the expressions for the spin–spin coupling tensor in the nonrelativistic limit can be derived.[5] Relativistic formulations of **J** have been derived. Aucar and Oddershede have formulated a fully relativistic ab initio theory of the spin–spin coupling in its most general form within the polarization propagator approach.[60] They neglect the Breit interaction to derive the formulas which look very much like the nonrelativistic expression for spin–spin coupling in the propagator approach, except that the elements involve integrals of the full four component wavefunctions. The large component of the relativistic wavefunction is the nonrelativistic wavefunction. One relativistic expression replaces the nonrelativistic $\mathbf{J}^{(OP)}$, $\mathbf{J}^{(SD)}$, and $\mathbf{J}^{(FC)}$ terms. Ramsey's nonrelativistic expressions are obtained in the limit that the speed of light goes to infinity. Kutzelnigg has also developed a relativistic theory of spin–spin coupling.[59] Earlier, Pyykkö derived a relativistic analog to Ramsey's theory, using a relativistic nuclear Zeeman hyperfine Hamiltonian as a perturbation.[11] Implementation of Pyykkö's theory has been limited to one-bond couplings.[61]

3 CALCULATIONS OF NUCLEAR MAGNETIC RESONANCE CHEMICAL SHIFTS

3.1 Comparison of Various Computational Methods Using the Same Set of Test Molecules

Which method would be best to use for calculating NMR chemical shifts? The answer depends on the question being asked. Is the chemical shift to be used to discriminate between two or more proposed chemical structures? Is the goal to verify a particular structure? Is it to determine if the molecule is fluxional or not, if forming a complex or not, on the basis of the NMR chemical shifts? Is it to assign the multitude of peaks observed in a crystalline sample? Sometimes we just want to understand what it is about the electronic structure that gives rise to an observed chemical shift or its temperature dependence. Depending on the accuracy that is required to answer the question being asked, a particular method and level of calculation and a particular size of basis set may be sufficient. It is not always necessary to use the most accurate method and the largest basis set. But first, we will compare methods across the board, using several benchmark molecules, in order to see the level of accuracy that may be expected.

We present some comparisons of absolute isotropic shieldings calculated using GIAOs in Tables 1 and 2. The calculations are for a fixed geometry, and therefore should be compared with the value for the equilibrium geometry

Table 1 Comparison between absolute shielding calculations, all using GIAOs and experiment[a]

Method	^{13}C in CH_4	^{13}C in CO	^{13}C in HCN	^{15}N in NH_3	^{15}N in N_2	^{15}N in HCN
DFT/BLYP[b]	184.33	−15.35			−84.82	
DFT/BLYP[c]	187.5	−17.7		259.2	−87.9	
DFT/BLYP[d]	187.80	−12.27	71.74	259.42	−80.55	−43.47
DFT/BLYP[e]	191.2	−9.3	91.5	262.0	−72.9	8.4
SCF[f]	194.8	−25.5	70.9	262.3	−112.4	−50.7
MBPT(2)[f]	201.0	10.6	87.6	276.5	−41.6	−0.3
MBPT(3)[f]	198.8	−4.2	80.0	270.1	−72.2	−26.2
MBPT(4)[f]	198.6	4.1	84.3	269.9	−60.1	−14.9
MCSCF	198.2[g]	8.22[g]	86.76[h]		−52.2[g]	2.63[h]
CCSD[i]	198.7	0.8	84.1	269.7	−63.9	−16.7
CCSD(T)[i]	198.9	5.6	86.3	270.7	−58.1	−13.6
Expt. σ_0^j	195.1 ± 1.2	1.0 ± 0.9	82.1 ± 0.9	264.5 ± 0.2	−61.6 ± 0.2	−20.4 ± 0.2
Expt. σ_e^k	198.7 ± 1.2	3.2 ± 0.9	84 ± 1	273.3 ± 0.2	−59.6 ± 0.2	−15 ± 1

[a] σ_e values are the ones that should be compared with the calculations. All shielding values are in ppm.
[b] Lee et al.[38]
[c] Cheeseman et al.[49]
[d] Rauhut et al.[48]
[e] Schreckenbach and Ziegler.[46]
[f] Gauss,[17]
[g] Ruud et al.[13]
[h] Barszczewicz et al.[21]
[i] Gauss and Stanton.[20]
[j] These are absolute shielding values σ_0 which are isotropic averages in the gas at the zero-pressure limit. They correspond to the thermal average for an isolated molecule. The error bars are associated with the determination of the absolute scale based on spin rotation constants for specific molecules (the CO molecule for ^{13}C, NH_3 for ^{15}N).
[k] The estimates of the vibrational corrections have been subtracted from σ_0 to obtain the value σ_e (the value for a rigid isolated molecule at its equilibrium molecular geometry) with which calculations are to be compared. See Jameson[62] for the references for experimental data and vibrational corrections.

of the molecule, σ_e, whereas the room temperature average value in the limit of zero density, $\sigma_0(300\,K)$, is for a rotating vibrating molecule. Electron correlation effects on the individual components of the tensor differ and so are partly washed out in the isotropic average value (which is one-third the sum of the principal components of the tensor). Nevertheless, these comparisons are revealing. Here we included the various levels of many body perturbation expansion MBPT(2), MBPT(3), MBPT(4) used by Gauss,[17] the coupled cluster approach for the singles and doubles approximation (CCSD)[19] and augmented by a correction for triple excitations (CCSD(T))[20] by Gauss and Stanton, a FCI calculation for BH molecule by Gauss and Ruud,[22] and the MCSCF results using GIAOs from Ruud et al.[13,21] We also include the results from DFT using the exchange functional of Becke with the correlation functional of Lee–Yang–Parr DFT/BLYP from calculations using the different implementations of Lee et al.[38] Cheeseman et al.[49] Pulay et al.[48] and Schreckenbach and Ziegler.[46]

Examination of Tables 1 and 2 permit the following conclusions. For the hydrides HF, H_2O, NH_3 and CH_4, electron correlation effects described by triple excitations are small, amounting to less than 1 ppm for the nonhydrogen nuclei. The effects for proton shieldings are not shown in the tables, but they are even smaller, of the order of 0.1 ppm. MBPT(4), CCSD and MCSCF all provide an adequate treatment of electron correlation effects for these simple systems. Furthermore, the agreement with experiment is very good. It has been suggested that these calculations are good enough to be able to say that the ^{17}O shielding scale (which has an error bar of ±17.2 ppm) may actually be closer to the less shielded edge of the error limits. It has been found in systematic studies of a large number of ^{13}C chemical shifts that MBPT(2)-level results are much closer to experiment than CCSD results.[64] It appears that MBPT(2) benefits from a fortuitous but consistent error cancellation, while CCSD (which is theoretically more complete and is in principle a more reliable approach) does not. Triplet excitation effects are considerably more important for the multiply bonded systems CO, N_2 and HCN. The magnitude of the triplet excitation corrections (2–6 ppm) for these systems leads to calculated results that are closer to experiment. For the F_2 molecule, inclusion of triple excitation corrections leads to a change of about 15 ppm and brings the calculated value closer to experiment. Results for F_2 at lower levels of calculation do not provide satisfactory agreement with experiment. Except for F_2 molecule, GIAO/MCSCF calculations using very large active spaces (only those are shown in Tables 1 and 2) provide results comparable to CCSD. It has been found,

For references see page •••

Table 2 Comparison between absolute shielding calculations, all using GIAOs and experiment[a]

Method	^{17}O in H_2O	^{17}O in CO	^{19}F in HF	^{19}F in F_2	^{1}H in BH	^{11}B in BH
DFT/BLYP[a]	317.86	−77.14	405.05	−271.70		
DFT/BLYP[b]	324.8	−80.7				
DFT/BLYP[c]	326.37	−73.60	410.87	−277.14		
DFT/BLYP[d]	331.5	−68.4	412.5	−282.7		
SCF[e]	328.1	−87.7	413.6	−167.9	24.21	−261.25
MBPT(2)[e]	346.1	−46.5	424.2	−170.0	24.12	−220.67
MBPT(3)[e]	336.7	−68.3	417.8	−176.9	24.14	−201.92
MBPT(4)[e]	337.5	−52.0	418.7	−174.0	24.22	−184.18
MCSCF[f]	335.3	−38.92	419.6	−136.6		−174.83[g]
CCSD[h]	336.9	−56.0	418.1	−171.1	24.74	−166.64
CCSD(T)[h]	337.9	−52.9	418.6	−186.5	24.62	−170.46
FCI[i]					24.60	−170.08
Expt. σ_0^j	344.0 ± 17.2	−42.3 ± 17.2	410.0 ± 6	−232.8 ± 6		
Expt. σ_e^k	357.6 ± 17	−36.7 ± 17	419.7 ± 6	−192.8 ± 6		

[a] σ_e values are the ones that should be compared with the calculations. All shielding values are in ppm.
[b] Lee et al.[38]
[c] Cheeseman et al.[49]
[d] Rauhut et al.[48]
[e] Schreckenbach and Ziegler.[46]
[f] Gauss.[17]
[g] Ruud et al.[13]
[h] van Wüllen.[63]
[i] Gauss and Stanton.[20]
[j] Gauss and Ruud[22]
[k] These are absolute shielding values σ_0 which are isotropic averages in the gas at the zero-pressure limit. They correspond to the thermal average for an isolated molecule. The error bars are associated with the determination of the absolute scale based on spin rotation constants for specific molecules (the CO molecule for ^{13}C, NH_3 for ^{15}N).
[l] The estimates of the vibrational corrections have been subtracted from σ_0 to obtain the value σ_e (the value for a rigid isolated molecule at its equilibrium molecular geometry) with which calculations are to be compared. See Jameson[62] for the references for experimental data and vibrational corrections.

and is obvious in Tables 1 and 2, that the DFT method consistently overestimates the paramagnetic term leading to too much deshielding for these benchmark molecules. The SCF value is good enough for CH_4, NH_3, and HF molecules to agree reasonably with the thermal average value (since the neglect of electron correlation effects in these and most molecules is compensated for by the neglect of rovibrational averaging), whereas this level of theory is clearly inadequate for the multiply bonded CO, HCN, and N_2, and also for H_2O and F_2.

The benchmark test molecules shown in Tables 1 and 2, except for CH_4, are specifically chosen as examples that presented problems of electron correlation, especially in ^{15}N, ^{17}O, and ^{19}F shielding. Observe in Tables 1 and 2 the slow convergence in some molecules, faster in others, of the series SCF, MBPT(2), MBPT(3), MBPT(4). Observe also the consistent improvement over SCF afforded by the approximate exchange correlation functionals used in DFT calculations especially for CO, N_2, HCN. Observe also how close CCSD(T) results come to the FCI (in BH molecule). More typical of the applications of calculated NMR chemical shifts to analysis of mixtures are calculations of ^{13}C chemical shifts. Table 3 demonstrates the importance of electron correlation to ^{13}C chemical shifts in the comparison with chemical shifts in the gas phase at the low density limit. It can be seen that the second order electron correlation generally brings the calculations close enough to experiment to be useful for analysis.

3.2 Comparison of Carbon Chemical Shift Tensor Components with Calculations

A more stringent test of the calculations has to do with reproducing the elements of the shielding tensor, not just the isotropic average that is obtained in solution or in a MAS experiment in the solid state. In a single crystal study of a sugar, for example, there are a large number of peaks which have to be assigned in order to verify the structure. Complete assignment of ^{13}C shielding tensors in the entire molecule from single crystal studies has been developed to the highest level by Grant et al. The multiple axis sample reorientation mechanism developed in this group permits the study of crystals containing 50–100 magnetically different nuclei per unit cell. In a polycrystalline solid with a very large number of distinct ^{13}C chemical sites, it is possible, using multidimensional NMR techniques to obtain the individual shielding tensor

Table 3 Calculated ^{13}C chemical shifts, in ppm relative to $^{13}CH_4$, and experimental values in the gas phase

Method A	$\sigma(CH_4) - \sigma(A)$, Calculated		Expt.[b]
	SCF[a]	MBPT(2)[a]	
CH_3CH_3	11.7	13.5	14.2
$H_2C{=}CH_2$	135.8	130.3	130.6
$HC{\equiv}CH$	81.8	78.2	77.9
CH_3F	71.6	79.7	78.3
CH_3OH	52.0	59.3	58.5
CH_3NH_2	31.9	36.6	36.8
CH_3CHO	33.5	38.7	37.9
$(CH_3)_2CO$	32.2	37.0	37.1
CH_3CN	4.8	7.9	7.4
CO	224.9	190.4	194.1
CO_2	147.9	138.0	136.3
H_2CO	205.0	194.8	
CH_3CHO	211.3	200.3	201.8
$(CH_3)_2CO$	218.8	207.3	208.2
HCN	127.5	114.2	113.0
CH_3CN	135.1	125.4	121.3
$CH_2{=}C{=}CH_2$	240.0	227.5	224.4
$CH_2{=}C{=}CH_2$	81.7	80.6	79.9
CF_4	116.4	137.1	130.6
C_6H_6	140.6	137.5	137.9

[a] Gauss[16]
[b] Jameson and Jameson.[65]

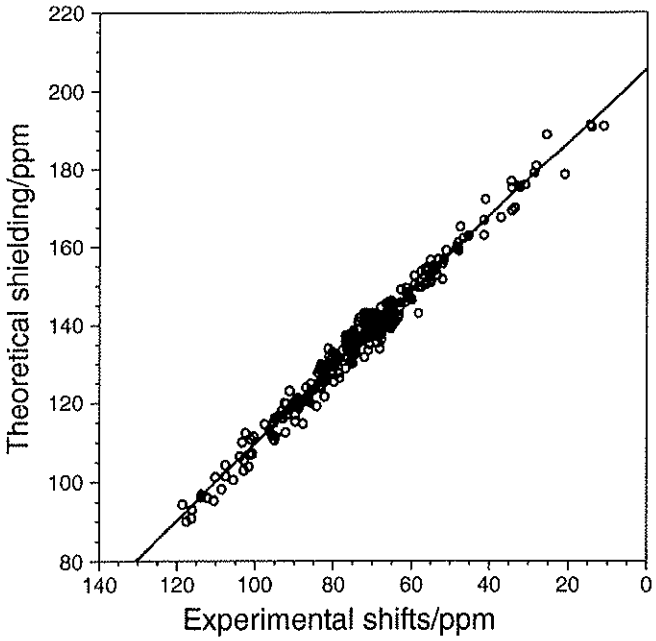

Figure 1 Comparison of computed full ^{13}C shielding tensors versus experimental values of icosahedral shift from TMS obtained from single crystal measurements. Both are expressed in the icosahedral representation that includes the principal axis system orientation. (Reproduced by permission from F. Liu, C.G. Phung, D.W. Alderman, D.M. Grant, *J. Am. Chem. Soc.*, **118**, 10 629–10 634. Copyright (1996) American Chemical Society.[67])

elements for each isotropic peak in the MAS NMR spectrum. To assign all these, ab initio calculations of shielding tensor elements are indispensable.

How well do calculations predict the tensor elements? It is important to be able to do these calculations in a relatively routine manner (one cannot use CCSD level of calculations) so that fitting to the observed spectra can be done expeditiously. Otherwise, theoretical calculations would not be practically useful for analysis. The group of D.M. Grant has carried out the largest number of such analyses.[66] Single crystal NMR experiments produce a complete description of the shielding tensor with six independent components specifying the tensor in a fixed crystallographic coordinate system (the so-called icosahedral tensor representation). Figure 1 shows the degree of success of SCF level calculations using a modest size basis set.[67] The high level of agreement between calculated and experimental tensors for ^{13}C is such that only the structural parameters (bond distances and angles) limit the level of agreement. This means that ab initio calculations and measurements together can be used to address certain fine details of solid state structure, surpassing the accuracy of X-ray data.[68] This is possible because the shielding tensor is exquisitely sensitive to bond distances.

It is quite important to be able to predict theoretically the individual tensor components of the building blocks of proteins, in order to establish that it is possible to use NMR chemical shifts in the determination of protein structure. In Figure 2 is the demonstration of the degree of success of SCF level calculations using a modest basis set for the tensor elements of ^{13}C in a single crystal of threonine.[69]

3.3 Other First Row Nuclei

A systematic study of B, N, O, and F shielding using the IGLO method of distributed origins provides a measure of the initial successes of theoretical calculations for these nuclei in systems of known structure.[7] ^{11}B NMR chemical shift calculations have been used for the analyses of new boron compounds, which are particularly useful when more than one structure can fit the electron diffraction data. Shielding calculations for N, O, and F in most molecules do require a theoretical treatment including electron correlation. Ab initio calculations for ^{17}O are of sufficiently high quality to indicate that the absolute shielding for ^{17}O in CO (used to define the experimental absolute shielding scale) is very likely at the lower edge of the reported error bars. DFT and ab initio methods have been used for ^{17}O shielding calculations in carbonyl complexes of transition metals (Ti, Zr, Hf, Fe, Rh, Cr, Mo, and W) by Kaupp et al.[70,71] and also

For references see page •••

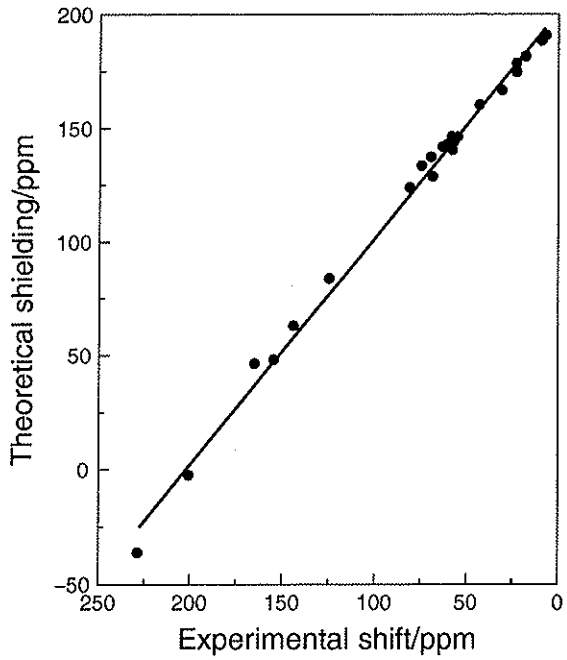

Figure 2 Comparison of computed full ^{13}C shielding tensors versus experimental values obtained from single crystal measurements for threonine. Both are expressed in the icosahedral representation that includes the principal axis system orientation. (Reproduced by permission from A.C. de Dios, D.D. Laws, E. Oldfield, *J. Am. Chem. Soc.*, **116**, 7784–7786. Copyright (1994) American Chemical Society.[69])

by Ziegler et al.[72] In using ^{17}O experiments to validate the calculations, the anisotropy of the tensor $(\sigma_{\parallel} - \sigma_{\perp})$ contains none of the uncertainty of the absolute shielding scale for ^{17}O and gives a good measure of the predictive success of ^{17}O calculations. Using this criterion, the DFT results agree with one of the crystalline sites in the symmetrical carbonyls $Cr(CO)_6$, and $Mo(CO)_6$, and differ by at least 10–20 ppm from the solid state experiments in $W(CO)_6$.

3.4 Second Row Nuclei

Systematic studies of the shielding of nuclei ^{29}Si, ^{31}P, ^{33}S and ^{35}Cl using IGLO distributed origins in a wide variety of molecules have been compared against chemical shifts, leading to reasonably good straight lines.[7] DFT calculations of ^{35}Cl shielding in XCl_4, where X = C, Si, Ge, Sn, and Ti gave good agreement with experimental chemical shifts observed in solution,[73] however, the calculations were not validated against any of the available absolute shielding, such as in ClF ($\sigma = -516 \pm 23$ ppm) or HCl ($\sigma = 952$ ppm). GIAO calculations including second order MP2 level electron correlation for ^{31}P has been used to estimate the infinite order results, and these agree very well with the absolute shieldings that are known for molecules ranging from PN to P_4 a range of about 900 ppm.[74]

3.5 Other Heavy Nuclei

Heavy nuclei present some general problems for calculations of NMR shielding. First, the larger number of electrons requires larger numbers of basis functions and including electron correlation becomes very expensive. Second, relativistic effects could be important. Third, in some cases there are few if any gas phase data that can be used to test the absolute shieldings from the calculations; in many cases, only solution-phase experimental data is available for comparison with calculations (e.g. ^{69}Ga, ^{115}In, ^{75}As, ^{121}Sb, ^{129}Xe). ^{77}Se is an exception to this third difficulty and can be used to explore the range of problems associated with heavy nuclei in general.

Correlation effects must be included for a quantitative description of ^{77}Se chemical shifts in those same bonding situations where ^{17}O shielding has been found to require correction for correlation effects. The additional complication of the large number of electrons therefore makes the ^{77}Se calculations more challenging. The results of ab initio calculations are very good. At the SCF level, for example, various calculations for the isotropic shielding of H_2Se lead to 2167.6, 2170, and 2171 ppm, which are very close to each other and reasonably close to the value calculated at the CCSD level (2213 ppm) and the experimental value: 2101 ± 64 ppm on the absolute shielding scale[75] (without the relativistic corrections for the diamagnetic shielding of the free atom). The electron correlation effects are only 2% of the total shielding in H_2Se and O=C=Se; they are 7% of the total shielding in Se=C=Se. This is very encouraging. Table 4 shows only the highest level ab initio calculations compared with DFT calculations and experiment. Keeping in mind that the rovibrational corrections are about −60 ppm, (that is, σ_e may be converted into experimental σ_0 by adding −60 ppm) the CCSD values are within 3–5% of the experimental values. The DFT results are less shielded than the CCSD values by 100–200 ppm.

The situation for ^{125}Te is comparable to that in ^{77}Se. ^{125}Te in TeF_6 gas has an absolute shielding of 2570 ± 130 ppm in the zero density limit, if the nonrelativistic diamagnetic shielding of the free atom is used. The DFT nonrelativistic calculations give 2260 ppm,[78] which is 200–300 ppm less shielded. This is in the same direction as the difference between DFT and CCSD in the ^{77}Se case. The ability of DFT calculations to reproduce the full range of ^{125}Te chemical shifts in all types of chemical bonding situation is very encouraging.[78]

3.6 Transition Metal Nuclei

For transition and post-transition metal nuclei there

Table 4 Calculated ^{77}Se shielding compared with experimental absolute shielding values in the gas phase (in ppm)

Molecule	$H_2C{=}Se$	Me_2Se	H_2Se	$O{=}C{=}Se$	$Se{=}C{=}Se$
CCSD σ_e^a	−741	1877.5	2213	2345	1596
DFT σ_e^b		1668	2093	2270	1441
Expt. σ_0^c	−900 ± 200	1756 ± 64	2101 ± 64	2348 ± 60	1610 ± 80

[a] Bühl et al.[76]
[b] Schreckenbach et al.[50]
[c] See Jameson[77] for the original sources of the experimental data.

are the usual problems associated with heavy nuclei, plus the lack of absolute shielding information. With one exception, there are no gas phase data to establish absolute shielding scales. Despite these problems some DFT calculations have been done for ^{103}Rh, ^{91}Zr, ^{57}Fe and ^{59}Co by Bühl and others. A relativistic formulation in which spin orbit contributions are neglected, resulting in the so-called scalar relativistic method is being explored within the DFT/GIAO method.[79] In calculations for other transition and post-transition metal nuclei for which the absolute shielding is not known, only shielding differences, i.e. chemical shifts, have been used to compare with experiment. The agreement is not yet at the level that is achievable routinely with ^{13}C shielding calculations. The range of transition metal shifts is usually very large and these exhibit useful diagnostic variations with ligand types. The theoretical calculations have yet to catch up with experiment. Witness for example, the one case where gas phase data is available: $CdMe_2$ molecule. Beam measurements show neat $CdMe_2$ liquid being deshielded by 1746 ppm from the free Cd atom, which has an absolute shielding of 4813 ppm. Thus $\sigma = 3067$ ppm for neat $CdMe_2$ liquid at room temperature. The gas is found to be 62.1 ppm unusually less shielded than the neat liquid,[80] so that $\sigma = 3005$ ppm for gaseous $CdMe_2$ at 97 °C. This is to be compared with 3504.5 ppm (too shielded by 500 ppm) from GIAO Cd shielding calculations on an isolated molecule of $CdMe_2$ with a spread of 105 ppm depending on basis set used, neglecting relativistic corrections or electron correlation.[81] Other calculations give more shielded values than this, as much as 900 ppm more shielded than 3005 ppm. Since the chemical shift range of Cd is about 900 ppm, the level of accuracy needs considerable improvement.

4 CALCULATIONS OF SPIN–SPIN COUPLING CONSTANTS

The various mechanisms in the nonrelativistic limit, given by Equations (10)–(14) are $\mathbf{J}^{(OD)}$, $\mathbf{J}^{(OP)}$, $\mathbf{J}^{(FC)}$, $\mathbf{J}^{(SD)}$, and the cross-term $\mathbf{J}^{(SDFC)}$ which has no isotropic part. The OD term, $\mathbf{J}^{(OD)}$, is the only term that is not expressed as a SOS in the Ramsey formulation, rather it is an average value of an operator containing two nuclear spins. $\mathbf{J}^{(OD)}$ is not usually small and can be rather large for ^2J(HH). A systematic study of this term shows that it is not very sensitive to basis set choice (double zeta with polarizations functions are sufficient) and to inclusion of electronic correlation (SCF average values will do); it is particularly important for ^nJ(HH), independent of n.[82] The sign of the contribution is negative for two-bond HH coupling. From a systematic study of the OP mechanism using DFT, $\mathbf{J}^{(OP)}$ appears to be significant for most couplings although not dominant, and is particularly important for couplings involving a nucleus with lone pairs.[83] The sign of the contribution (reduced so as to not include the nuclear gamma values) can be positive or negative; $\mathbf{J}^{(OP)}$ is negative and is the largest contribution for CO and N_2 molecules, for example. The SD term $\mathbf{J}^{(SD)}$ is the most time-consuming to calculate and so is sometimes neglected; it is not small when multiple bonds are involved between the coupled nuclei. For example, for N_2 molecule it is comparable to and partly cancels the $\mathbf{J}^{(FC)}$ term.[25,27,84] Electron correlation is very important for multiple bonded systems and must be accounted for to obtain reliable results: results at the RPA level have the wrong sign and magnitudes for coupling in both CO and N_2 molecules. The sign and magnitude of the FC, $\mathbf{J}^{(FC)}$, term varies across the periodic table. Where no multiple bonds are involved, this mechanism usually provides the largest contribution to one-bond coupling constants. Electron correlation is very important for this mechanism and unrealistic values may result from calculations at the RPA level.

4.1 One-bond Coupling Constants

Table 5 shows the various contributions to the one-bond couplings in HF, HCl, CO and N_2. The uncorrelated results (RPA) are shown to be inadequate. Various methods of including electron correlation are (1) through the polarization propagator approach to SOPPA and CCSD level, (2) MBPT, (3) MCLR theory, (4) DFT, and

For references see page •••

Table 5 One-bond spin–spin coupling constants (Hz)

Molecule	Method	Ref.	$J^{(FC)}$	$J^{(OP)}$	$J^{(OD)}$	$J^{(SD)}$	J	J, Expt.
HF	RPA	85	467.3	119.3	−0.1	−12.4	654.1	
	SOPPA	85	338.3	195.7	−0.1	−1.0	532.9	
	MBPT	86	390.71	195.14	1.69	−17.47	570.01	
	CCSD/PPA[a]	85	329.4	195.7	−0.1	−0.6	524.4	
	DFT	87	198.1	198.0	0.1		396.2	
	EOM/CCSD	27	338.2	176.2	0.0	−1.0	513.4	529 ± 23
$H^{35}Cl$	RPA	27	16.78	13.70	0.00	−0.45	30.03	
	MBPT	86	12.52	12.02	0.00	−0.08	24.45	
	EOM/CCSD	27	22.04	12.65	0.00	0.34	35.03	37.7
$^{13}C^{17}O$	RPA	25	−8.1	12.2	0.1	−9.3	−5.1	
	SOPPA	25	7.3	14.8	0.0	−4.0	18.1	
	MCLR	84	6.69	13.66	0.09	−4.33	16.11	
	DFT	87	13.4	12.4	0.1		25.9	
	EOM/CCSD	27	7.0	13.0	0.1	−4.6	15.5	16.4 ± 0.1
$^{14}N^{15}N$	RPA	25	−7.65	0.50	0.0	−8.13	−15.26	
	SOPPA	25	0.45	3.25	0.0	−1.55	2.18	
	MCLR	84	−0.23	2.83	0.02	−1.85	0.77	
	DFT	87	2.0	2.7	0.0		4.7	
	EOM/CCSD	27	0.3	2.8	0.02	−1.7	1.4	1.8 ± 0.6

[a] PPA, Polarization Propagator Approximation.

(5) EOM/CCSD. The DFT calculations suffer from the inadequacy of the approximate exchange correlation functionals available. These functionals may be good enough to reproduce binding energies, but offer less accurate descriptions of the electron spin distributions where they are needed in calculations of **J**, especially the FC mechanism. MCLR theory uses an MCSCF reference state and is capable of describing electronic systems with large static correlation effects.

How well do calculations predict the simple one-bond ^1J(CH)? This may be observed in Table 6, where it is seen that the isotropic value is entirely dominated by the FC mechanism and is easily reproduced by calculations that include correlation, including DFT. Correlation effects can be substantial. For example, the uncorrelated calculation of the term FC for ^1J(CH) in HCCH molecule leads to 449.3 Hz, whereas SOPPA which includes correlation up to second order gives 246.5 Hz, which agrees quite well with the experimental value of 248.7 Hz.

On the other hand, calculations are less successful with the one-bond ^1J(CF). DFT is found to underestimate the FC contribution to the one-bond coupling because of the inability of such exchange correlation functionals

Table 6 One-bond CH coupling constants, ^1J(CH) (Hz)

Molecule	Method	Ref.	$J^{(FC)a}$	J	J, Expt.
CH_4	CCSD/PPA	26	122.12	123.87	120.78 ± 0.05[b]
C_2H_4	EOM/CCSD	88	145.63	147.66	156.4
HCCH	SOPPA	24	246.5	246.5	248.7
CH_3F	EOM/CCSD	88	136.44	137.89	149.1
CH_3CN	EOM/CCSD	88	123.29	125.69	136.0
CH_3NH_2	EOM/CCSD	88	120.88[c]	123.29[c]	132.5
Cyclopropene	MCSCF	89	163.6	164.7	167
Cyclopropene	MCSCF	89	212.7	213.1	226
Cubane C_8H_8	EOM/HRPA	90	145.62	146.45	154.5
CH_4	DFT	87	122.0	123.9	120.78 ± 0.05[b]
C_2H_4	DFT	42		153.9	156.4
CH_3CH_3	DFT	42		123.87	124.9
HCCH	DFT	42		250.8	248.7

[a] The FC contribution only.
[b] This value, corresponding to the equilibrium structure, is obtained after the experimental value is corrected for rovibrational averaging. All other experimental values are uncorrected thermal averages at room temperature.
[c] Average values.

to produce the accurate spin densities required for this calculation. In the presence of polarizable lone pairs the correlation problem is more severe and the available functionals do not describe the spin densities well enough in the case of ^1J(CF) which are predicted to be about 110 Hz away from experimental values, as shown in Table 7.

There are many interesting trends observed in coupling constants, in signs, magnitudes, dependence on substituents, stereochemistry, position of coupled nuclei in the periodic table, and so on.[91] Many of these trends have been very useful in analysis of spectra and yet a sound theoretical basis for few of such trends has been established.

The anisotropy of the tensors calculated with and without electron correlation are shown in Table 8 for HF and HCl.[86] First of all, note that the FC mechanism is purely isotropic and the cross-term $\mathbf{J}^{(SDFC)}$ which has no isotropic part, is responsible for a large part of the total anisotropy of the tensor. The anisotropy of the orbital mechanisms are opposite in sign and partly canceling. The contribution to the anisotropy from the SD mechanism is small. Any anisotropy observed in the **J** tensor in oriented molecules has to come from the mechanisms other than the FC term. However, because of the very large contribution from the cross-term $\mathbf{J}^{(SDFC)}$ to the anisotropy (78% in HF and 93% in HCl), the magnitude of the measured anisotropy unfortunately conveys very little information about the magnitude of the contributions of mechanisms other than the FC term to the isotropic average observed in solution. The effect of electron correlation on the individual components of $\mathbf{J}^{(OD)}$ is small. (It is well known that the effect of correlation on the isotropic average of $\mathbf{J}^{(OD)}$ is small and that it is not very sensitive to basis set choice.) The orbital mechanisms have opposite contributions to the anisotropy, $\mathbf{J}_{\parallel}^{(OD)}$ and $\mathbf{J}_{\perp}^{(OP)}$ are similar in sign (positive) and magnitude (large), and so are $\mathbf{J}_{\parallel}^{(OP)}$ and $\mathbf{J}_{\perp}^{(OD)}$ (negative and smaller). The effect of electron correlation on the cross-term $\mathbf{J}^{(SDFC)}$ is about 5%. If this is typical, uncorrelated calculations should permit estimation of the **J** anisotropy that may be expected in oriented systems. There are only a few measurements of the anisotropy of the **J** tensor because the observable quantity in solids is the (**D** + **J**) tensor, and the direct dipolar coupling tensor **D** overwhelms the sum. The anisotropy of the **J** tensor has been determined in a few favorable cases, such as $^1J(^{31}P{-}X)$, where $X = {}^{199}Hg$, ^{95}Pt, ^{115}In, in Wasylishen's laboratory.[92] A typical such measurement in a single crystal of a mercury phosphine complex shows the experimental technique for arriving at $\mathbf{J}_{\parallel} = 11800$ Hz, $J_{\perp} = 6400$ Hz, and the isotropic value is 8200 Hz. While the isotropic value is very likely to be dominated by the FC mechanism, the anisotropy $\Delta\mathbf{J} = 5400$ Hz comes entirely from the non-FC mechanisms.[92]

Table 7 One-bond CF coupling constants, ^1J(CF) (Hz)

Molecule	Method	Ref.	Calculated	Expt.
CH_3F	EOM/CCSD	88	−172.37	−157.5 ± 0.2
CH_3F	DFT	52	−268.12	−157.5
CH_2F_2	DFT	52	−343.11	−234.8
CF_4	DFT	52	−379.37	−259.2
CH_3CF_3	DFT	52	−379.06	−271
CHF_3	DFT	52	−390.72	−274.3
$CHCl_2F$	DFT	52	−388.50	−293.8
CF_3Cl	DFT	52	−415.33	−299
F_2CO	DFT	52	−426.22	−308.4
$CFCl_3$	DFT	52	−448.83	−337
FC(O)H	DFT	52	−455.01	−369
F_2CSe	DFT	52	−510.87	−408

Table 8 Contributions to the calculated anisotropy of the one-bond coupling, $\Delta\mathbf{J} = (\mathbf{J}_{\parallel} - \mathbf{J}_{\perp})$ (Hz)[a]

		$\mathbf{J}^{(FC)}$	$\mathbf{J}^{(OD)}$	$\mathbf{J}^{(OP)}$	$\mathbf{J}^{(SD)}$	$\mathbf{J}^{(SDFC)}$	Total
HF, SCF	$\mathbf{J}_{\parallel}$	453.44	143.50	−11.34	−71.96	−392.22	121.41
	$\mathbf{J}_{\perp}$	453.44	−69.43	297.82	0.44	196.11	878.38
	$\Delta\mathbf{J}$	0	212.93	−309.16	−72.4	−588.33	−756.97
HF, MBPT(2)	$\mathbf{J}_{\parallel}$	390.71	143.12	−8.92	−58.78	−373.40	92.73
	$\mathbf{J}_{\perp}$	390.71	−69.03	297.17	3.18	186.63	808.65
	$\Delta\mathbf{J}$	0	212.15	−306.09	−61.96	−560.03	−715.92
HCl, SCF	$\mathbf{J}_{\parallel}$	25.17	13.19	−2.90	−2.33	−42.26	−9.14
	$\mathbf{J}_{\perp}$	25.17	−6.60	18.95	0.71	21.13	59.36
	$\Delta\mathbf{J}$	0	19.79	−21.85	−3.04	−63.39	−68.50
HCl, MBPT(2)	$\mathbf{J}_{\parallel}$	12.52	13.19	−2.52	−1.84	−41.38	−20.03
	$\mathbf{J}_{\perp}$	12.52	−6.59	19.29	0.80	20.68	46.70
	$\Delta\mathbf{J}$	0	19.78	−21.81	−2.64	−62.06	−66.73

[a] Fukui et al.[86]

For references see page •••

4.2 The Two-bond Coupling Constant

The geminal coupling constant ^2J(HH) turns out to be very difficult to predict. As is the case for all ^nJ(HH), the $\mathbf{J}^{(OD)}$ term is important. So also is the $\mathbf{J}^{(OP)}$ term, but it has the opposite sign to the $\mathbf{J}^{(OD)}$ term. For the series CH_4, SiH_4, GeH_4, SnH_4, the orbital mechanism $J^{(OD)}$ and $J^{(OP)}$ terms have opposite signs and they very nearly cancel in CH_4. The magnitude of the $\mathbf{J}^{(FC)}$ term varies from large negative to large positive. There is poor agreement of the total calculated value with experiment.[31] The experimental variation of ^2J(HH) with the nature of the intervening atom is not predicted quantitatively, although the trend of algebraically increasing from C to Sn is reproduced at every level of correlation treatment.[31,52] In the series CH_4, NH_3, OH_2, ^2J(HH) has the sign of the $\mathbf{J}^{(FC)}$ term, but is by no means dominated by it. Here too, the experimental variation of ^2J(HH) with the position of the intervening atom in the periodic table is not predicted quantitatively, although the trend of algebraically increasing from C to N to O is reproduced at every level of correlation treatment.[27]

4.3 Coupling Over Three-bonds

From a practical viewpoint, one of the very early major successes of theoretical calculations of spin–spin couplings is the prediction of the torsion angle dependence of ^3J(HCCH), known as the Karplus equation. The very simple valence bond calculation[93] using a small four-atom fragment (HCCH) led to an unequivocal prediction which permitted a practical determination of structure strictly from the observed isotropic value of the coupling constant. It was found later that the dihedral angle dependence of the three-bond coupling is general and Karplus-type equations have been used to describe many types of three-bond coupling pathways, for example ^3J(X–Y–C–H), where X represents other nuclei such as ^{31}P or ^{13}C or ^{15}N, and three-bond coupling paths such as PtCCC, PWNN, PCPSe, etc. Used with caution, experimental ^3J values and a Karplus equation make a reasonable conformational probe. The original Karplus equation is written in the form of Equation (19)

$$^3J(\mathrm{HCCH}) = C_0 + C_1 \cos\phi + C_2 \cos(2\phi) \qquad (19)$$

with $C_0 = 8.02$, $C_1 = -1.2$, and $C_2 = 7.0$ Hz as the empirical parameters, although other forms have also been used. The coefficients in the above equation have been calculated by various methods using ethane as the model. The $\mathbf{J}^{(FC)}$ contribution is the largest and $\mathbf{J}^{(SD)}$ the smallest. One such calculation, with second order correlation for all contributions except the FC contribution (which was done with third order correlation), leads to $C_0 = 4.66$, $C_1 = 0.39$, and $C_2 = 5.78$ Hz.[94] In the general case, the ^3J value also depends on the bond angles between any two adjacent bonds out of the three, and there are substituent effects.

4.4 Relativistic Effects

Why are relativistic effects important for spin–spin couplings of heavy nuclei? Relativistic effects are particularly important for electronic properties which depend on the electronic wavefunctions very near nuclei where electrons move fast. Relativistic effects on the electronic structure of atoms and molecules consist of a contraction of s and p shells, the spin–orbit splitting of the non-s shells and the relativistic SCF expansion of d and f shells. The contraction of the s and p shells leads to larger spin densities at the nuclei (FC term) and also larger values of $\langle r_{kN}^{-3} \rangle$ (other mechanisms). An a posteriori correction of the nonrelativistic values of these by a multiplicative factor $B(n, Z)$, depending on the principal quantum number n and the nuclear charge Z, was suggested by Breit in 1930[95] and this multiplicative factor has been used by Pyykkö and others to impose a simple relativistic correction on the values of J calculated using the nonrelativistic formulas.[96] This factor, $B(n, Z)$, is 1.348 for the $n = 5$ shell of Sn and is 2.592 for the $n = 6$ shell of Pb.[96] That is, the nonrelativistic calculations underestimate the value of J(SnH) by a factor of 1.348. When both nuclei involved in the coupling are heavy, the product of two such factors is substantial.

5 CALCULATIONS OF ELECTRIC FIELD GRADIENTS

5.1 Electric Field Gradient Tensor Versus Electronic Structure in the Solid State

The electric field gradient tensor is intimately related to the local molecular structure. In crystalline silicates, for example, the measured ^{17}O nuclear quadrupole coupling constant serves as a probe of oxygen coordination number and geometry. Using experimental correlations between structure (Si–O–Si bond angles, for example) in crystalline silicates and the measured ^{17}O quadrupolar coupling constants, the Si–O–Si bond angle distribution in silicate glasses can be deduced, bridging and nonbridging oxygens can be distinguished.[97] Electric field gradient tensors of deuterium nuclei in hydrogen bonded positions, such as the amide or carboxy hydrogen in peptides, give deuteron/proton bond directions with an accuracy rivaled only by neutron diffraction, since it has been established that the unique eigenvector of a deuteron quadrupole coupling tensor is approximately parallel to the bond direction of the deuteron.[98]

5.2 Calculations of Electric Field Gradients at Nuclei in Isolated Small Molecules

The most reliable method of obtaining the intrinsic electric quadrupole moment of a nucleus is by very high quality ab initio calculations of the electric field gradient tensor in selected small molecules in which the nuclear quadrupole couplings of the nucleus have been measured accurately via microwave spectroscopy. The value of eQ is obtained as a fit parameter.[99] Once calibrated, this eQ value can be used to deduce from experiment the electric field gradient tensor for any other nuclear site.

Accurate theoretical calculations of electric field gradients for small molecules pose no special problems, requirements of basis set quality and appropriate level of electron correlation depend on the molecule, just as for calculations of shielding, but less demanding in that only the ground electronic wavefunction is required. Just as for shielding calculations, the r^{-3} factor in the electric field gradient requires wavefunctions that are accurate in the immediate vicinity of the nucleus.

5.3 Simulations of Nuclear Quadrupole Coupling in Associated Liquids

The presence of neighboring molecules influences the electric field gradient at a nuclear site, by directly providing additional charge distributions outside of the molecule and also by distorting the electronic distribution of the molecule of interest. An extreme case is a liquid in which hydrogen bonding or complex formation is present. One approach to the calculation is to consider the liquid as having a distribution of clusters of all sizes, monomers, dimers, n-mers where n is truncated at some value when the contribution to the average value is sufficiently small. Molecular geometries of each n-mer are optimized and the electric field gradients are calculated at each nuclear site in the n-mer. Molecular partition functions are calculated for each n-mer, and from thermodynamic calculations the distributions of the n-mers are obtained. The average electric field gradient for each cluster is weighted with the cluster distribution to obtain the electric field gradient values in the liquid phase. The ^{14}N, ^{17}O, and ^{2}H of the carbonyl and *cis* and *trans* amides have been calculated in liquid formamide by this method, for comparison with the experimental values of NMR quadrupolar relaxation time as a function of temperature.[100] Cyclic hexamers are found to be the dominant species at room temperature, consistent with structural data from neutron diffraction, low frequency Raman and far-infrared spectra. This method of calculation has been applied to liquid HCN, in which the calculated values for the isolated monomer, dimer, and trimer successfully predict the values known independently from pulsed Fourier transform microwave experiments on the van der Waals complexes.[101] Theoretical calculations such as these, combined with measurements of the nuclear quadrupole coupling constants as a function of temperature, can provide a useful general probe of electronic changes accompanying hydrogen bonding, cluster formation, solvation, phase condensation, and other phenomena in condensed media.

5.4 Relation Between Chemical Shift and Electric Field Gradient Tensors

NMR measurements in single crystals permit the independent determination of the principal axis systems of the electric field gradient tensor and the shielding tensor.[102] Even in the powder it may be possible to find the relative orientation of these two axis systems by referring to the known axis system for the dipolar coupling. The two axis systems are not necessarily coincident. Theoretical calculations of both the electric field gradient and the shielding tensors at the same nuclear site provide descriptions of the electronic distribution and chemical bonding which can be checked directly against experiment. They provide respectively, a measure of the bond direction and the strength of the hydrogen bond for the deuterium nucleus, for example. In materials that exhibit a distribution of nuclear sites, such as glasses or polymers, multidimensional solid state NMR techniques permit the determination of the anisotropic chemical shift as a function of the isotropic chemical shift or of the electric field gradient as a function of the isotropic chemical shift. From such measurements, the anisotropic chemical shift of ^{29}Si and the electric field gradient of ^{17}O nuclei, for example, can both be used to characterize a silicate glass or other complex material, providing complementary information.[103,104] Thus, these two tensors provide local electronic information even in complex materials. With the assistance of theoretical calculations such multidimensional solid state NMR experiments can provide answers to questions about the microscopic structure of solids, on the extent of order/disorder in cation environments, random distributions or amorphous/crystalline domains, short range and long range order, and so on.

6 INFLUENCE OF INTRAMOLECULAR GEOMETRY AND ENVIRONMENT ON NUCLEAR MAGNETIC RESONANCE PARAMETERS

The temperature dependence, mass dependence (isotope effects), and site sensitivity (dependence on secondary/tertiary structure of proteins, for example) of chemical shifts, spin–spin couplings, and electric field gradients provide additional information about structure,

For references see page •••

dynamics, and environment of a molecule or a particular part of a molecule.

6.1 Nuclear Magnetic Resonance Parameter Dependence on Local Geometry: Bond Lengths, Bond Angles, Torsion Angles

The insight into structure and environment provided by the NMR chemical shift is obtained by a combination of theoretical calculations and experiments.[105] The NMR chemical shift discriminates between the various alanine residues in the same protein molecule, between two nuclear sites identical in every way except that one has ^{18}O in a neighboring bond rather than ^{16}O (isotope shift studies), between a ^{15}N (and ^{13}C) in a dynamically averaged rather than rigid headgroup at an oriented membrane interface, for example. In most cases, theoretical calculations using innovative model fragment systems are required to interpret the relation between the structure and the chemical shift. The discrimination is afforded by the extreme sensitivity of the shielding tensor to the local geometry: the bond lengths, bond angles, and torsion angles. The mathematical surface describing the shielding tensor as a function of these geometrical parameters is called a shielding surface. Vibrational averaging over the shielding surface, weighted by the probabilities of finding the molecule at the geometries described by these parameters (the vibrational wavefunction provides these probabilities) gives average shielding values that are different for different isotopomers, gives average shielding values that are different for particular (ϕ, ψ) angles that characterize particular alanine residues in a protein. Thus, isotope effects on chemical shifts can be predicted; the distinguishing chemical shifts of different alanine residues in a protein can be associated with specific local conformations, leading to structure determination. The application of quantum mechanical calculations of shielding surfaces to the structural characterization of proteins was introduced by de Dios, Pearson, and Oldfield.[106] This approach has led to the possibility of secondary and tertiary protein structure determination from NMR chemical shifts in solution using ^{13}C alone.[107] The method is extremely powerful when combined with complementary information obtained from geometry sensitivity of other NMR parameters such as spin–spin coupling and ^{1}H chemical shifts.[108] The use of theoretical calculations of NMR shielding surfaces to elucidate structure and dynamics finds application in the gas phase, in catalysis, as well as in biomolecular systems.[105,109,110]

The dependence of the spin–spin coupling, the electric field gradient and other molecular electronic properties on bond lengths and bond angles, and the observations that are the experimental manifestation of this, are similar to that discussed above for shielding. The general theoretical basis for isotope effects and temperature dependence of these properties is the same. With the assumption of the Born–Oppenheimer separation of nuclear motion from electronic motion, the mathematical surface describing the dependence of **J** (or other) on the geometrical parameters (such as bond lengths) exists, just as does as the potential energy surface of the molecule. Averaging on the property surface is according to the probability of finding the molecule at various geometries, which in turn is determined by the vibrational wavefunctions corresponding to the potential energy surface.[111] Raynes et al. have provided very good case studies of these effects on coupling constants in polyatomic molecules, including details of the theoretical surfaces, dynamic averaging, and experimental measurements of the temperature dependence of spin–spin coupling in the various isotopomers.[112–115]

6.2 Intermolecular Effects

NMR shielding is extremely sensitive to intermolecular effects. This sensitivity is manifested by the very large gas-to-liquid shifts (4.4 ppm for ^{1}H in H_2O, 19.5 ppm for ^{15}N in NH_3, 77 ppm for ^{31}P in P_4, 120 ppm for ^{77}Se in H_2Se, around 200 ppm for ^{129}Xe in xenon), by the aromatic solvent-induced proton chemical shifts, and by the very large average chemical shifts observed for Xe in various media such as zeolites and polymers.[105,110] Theoretical calculations of these intermolecular effects are sometimes carried out by approximating the medium as a continuum and considering the molecule in a cavity within this medium of fixed dielectric constant. Such an option is routine in many quantum mechanical software packages. Another approach is to consider the intermolecular effects in terms of electrical polarization effects of fixed partial electrical charges centered on surrounding atoms in a crystalline system. A more complete treatment is to calculate the nuclear shielding in the molecule together with the solvent at various internuclear separations and orientations and then to average such shieldings over the appropriately weighted configurations at each temperature.[116,117] The effects of hydrogen bonding on the ^{1}H shielding tensor in ice have been reproduced by calculations using 17 H_2O molecules arranged in the experimental ice configuration, for example, emphasizing the importance of long range effects.[118] While the short range effects on shielding of ^{13}C, ^{15}N, ^{17}O and ^{1}H nuclei in each amino acid residue protein (the geometry dependence and hydrogen bonding) can be calculated using a model fragment, the long range effects of neighboring residues may be considered in the same way as intermolecular effects from solvent molecules. It has been found that such long range electrostatic effects have an important role to play in interpreting ^{1}H,

^{15}N and ^{17}O chemical shift inequivalencies in proteins, and neighbor anisotropy has an important role in the case of ^{1}H. Molecular dynamics (MD) has been used to produce a large number of instantaneous configurations for which the component magnitudes and directions of the ^{15}N shielding tensor can be calculated in a simple model system (three *N*-methylacetamide complexes) constructed from a gramicidin channel in a fully hydrated phospholipid bilayer.[119] The MD method of sampling reveals fluctuations in the tensor properties which may be used to investigate the types of NMR spectra produced during such motional averaging for a protein observed in a fluid bilayer environment.

A clear case of intermolecular effect on chemical shifts is found in the xenon atom. The use of ^{129}Xe chemical shifts in studies of various electronic environments (zeolites, polymers, clays, coals, biological systems) depends on theoretical calculations of the intermolecular effects on ^{129}Xe shielding in the xenon atom. The dispersion of the Xe signal in these various media is very useful as a diagnostic tool in the analysis of structure of the medium, the distribution of Xe atoms within, and the rate of exchange (diffusion) of Xe from one cage (or channel or domain) to another, as well as from within the medium to the bulk phase. The ability to reproduce the temperature dependence of the intensities and the individual chemical shifts in the ^{129}Xe NMR spectrum of the various Xe_1, Xe_2, Xe_3, . . ., Xe_8 signals observed for xenon trapped in variety of *A* zeolites, (Na*A*, $Ca_xNa_{12-2x}A$, K*A*, Ag*A*) using a combination of quantum mechanical calculations and statistical mechanical averaging,[117,120-123] permits the interpretation of the NMR observations in various other zeolites wherein fast xenon exchange leads to one signal that contains the average over all distributions.[124] The Xe chemical shifts are very large (several hundred ppm) and discriminate between amorphous and crystalline regions in polymers and coals; however, the theoretical prediction of the Xe NMR spectrum in these more complex materials lags behind the experiments. The same approach as used in the crystalline zeolites should work in these more complex systems, provided that an appropriate model system can be introduced and tested in each case.

Theoretical approaches for intermolecular effects on **J** would be the same as for chemical shifts, although the observed effects are generally smaller. Intermolecular effects on electric field gradients at a nucleus can be substantial. In van der Waals dimers and higher *n*-mers, the nuclear quadrupole coupling constant can be sufficiently different from that found in the monomer and can be used to deduce the structure of the clusters formed. Calculations of the electric field gradient at a nucleus in a cluster treated as a supermolecule generally have to be carried out as a function of geometry, and it is usually necessary for internal coordinates to be permitted to vary with intermolecular separation. Furthermore, consistent with the strength of intermolecular forces, cluster vibrations can be very anharmonic, so averaging will have to be done accordingly. Farrar and Weinhold have carried out averaging of the electric field gradient at the ^{14}N and ^{2}H nuclei of HCN in $(HCN)_2$ and $(HCN)_3$ and $(HCN)_n$ up to $n \approx 6$.[101] The interpretation of the nuclear quadrupole couplings in liquid HCN as a function of temperature also requires that the distribution of the dominant clusters be calculated by statistical mechanics. The nonpairwise additive cooperativity effects in the hydrogen bonding that are comparable in magnitude to that of dimer formation in this system cannot be neglected in the calculation of the NMR parameters. For the same reason, the NMR parameters of liquid water or ice cannot be deduced from calculations on $(H_2O)_2$ alone.

Many interesting materials analyzed by NMR spectroscopy are made up of covalent networks. Calculations of NMR parameters in extended networks is not yet tractable. One approach to calculations in such systems is to consider models consisting of truncated clusters. For example, ^{29}Si shielding, ^{17}O shielding and electric field gradients, and ^{27}Al electric field gradients in silicates and aluminosilicates are of great interest in the NMR analyzes of zeolite structure. Zeolites are aluminosilicates with crystalline structure which are constructed from SiO_4 tetrahedra joined together by sharing edges and vertices. Al may replace Si in the lattice, with the charge balanced by extra-framework cations. Thus, the crystal is formed by a network of Al/Si atoms connected by bridging O atoms. Some clusters that have been used in calculations of NMR parameters of zeolites include fragments of the sodalite cage terminated by H atoms replacing the truncated Al or Si atoms in the extended network, or by replacing the truncated bridging oxygen atoms by H atoms.[125,126] Another possible approach is the use of an embedded small fragment within the much larger cluster. The small fragment which consists of the nucleus of interest and its immediate neighbors, is treated ab initio quantum mechanically at an appropriate level, the rest of the atoms in the much larger truncated cluster carved out of the network being treated at a lower level (semiempirically or by molecular mechanics). Such hybrid approaches appear promising for extended covalent networks and polymers.

7 FUTURE DEVELOPMENTS

Theoretical calculations of shielding and electric field gradient tensors for isolated molecules are well in hand, except where relativistic effects are important. Relativistic

For references see page •••

calculations have yet to be carried out in a theoretically rigorous manner, rather than using a patchwork of spin-free and spin–orbit contributions. Heavy nuclei, particularly transition metal nuclei, which are important components of technologically important solid materials, cannot be treated accurately until the problem of relativistic effects is solved. The extreme sensitivity of shielding and electric field gradient tensors to intermolecular effects and local geometries (imposed by longer range order and distributions) presents a distinct advantage as well as difficulties. Applications of calculations of shielding and electric field gradients to interpretations and analyzes of complex systems require construction of appropriate useful models that can be tested in simpler systems and extended to complex ones. By separating the various short range (geometrical, hydrogen bonding) and long range intermolecular contributions to the chemical shift, a powerful tool in analyzing structure, dynamics, and environment can be realized. The approach used in proteins can be extended to other polymers and even mixtures of polymers. Theoretical calculations of spin–spin coupling constants are more difficult, even in isolated small molecules, but are slowly becoming more tractable. These have sensitivity to local geometries but are less susceptible to intermolecular effects and long range contributions. The use of density functional techniques offers hope that larger systems can be handled, but the difficulties with the presently available approximate exchange correlation functionals naturally limit the accuracy of the results that can be obtained. When more accurate functionals become available, this will clearly be the method of choice for very large systems.

ABBREVIATIONS AND ACRONYMS

BLYP	Becke–Lee–Yang–Parr
CAS	Complete Active Spaces
CSGT	Continuous Set of Gauge Transformations
CC	Coupled Cluster
CCSD	Coupled Cluster Singles and Doubles
CCSD(T)	Coupled Cluster Singles and Doubles with Some Triple Excitations
CHF	Coupled Hartree–Fock
CDFT	Current Density Functional Theory
DFT	Density Functional Theory
OD	Diamagnetic Orbital
EOM	Equation of Motion
FC	Fermi Contact
FCI	Full Configuration Interaction
GIAO	Gauge Including Atomic Orbitals
HRPA	Higher Random Phase Approximation
IGAIM	Individual Gauges for Atoms in Molecules
IGLO	Individual Gauge for Localized Orbitals
KSDFT	Kohn–Sham Density Functional Theory
LDA	Local Density Approximation
LORG	Localized Orbital/Local Origin
MAS	Magic-angle Spinning
BDFT	Magnetic Field Density Functional Theory
MBPT(n)	Many Body Perturbation Theory (nth order term)
MBPT	Many Body Perturbation Theory
MD	Molecular Dynamics
MCIGLO	Multiconfiguration Individual Guage for Localized Orbitals
MCLR	Multiconfiguration Linear Response
MCSCF	Multiconfiguration Self Consistent Field
MPn	Møller–Plesset (nth order term)
MP2	Møller–Plesset Second Order Term
NMR	Nuclear Magnetic Resonance
NOE	Nuclear Overhauser Effect
OP	Paramagnetic Orbital
PPA	Polarization Propagator Approximation
RPA	Random Phase Approximation
RAS	Restricted Active Spaces
MBPT(2)	Second Order Many Body Perturbation Theory
SOPPA	Second-order Polarization Propagator Approximation
SCF	Self Consistent Field
SD	Spin Dipolar
SOS	Sum Over States
TMS	Tetramethylsilane
UHF	Unrestricted Hartree–Fock

List of general abbreviations appear on back endpapers

REFERENCES

1. N.F. Ramsey, 'Magnetic Shielding of Nuclei in Molecules', *Phys. Rev.*, **78**(6), 699–703 (1950).
2. N.F. Ramsey, 'Chemical Effects in Nuclear Magnetic Resonance and in Diamagnetic Susceptibility', *Phys. Rev.*, **86**(2), 243–246 (1952).
3. N.F. Ramsey, 'Electron Coupled Interactions Between Nuclear Spins in Molecules', *Phys. Rev.*, **91**(2), 303–307 (1953).
4. F. Michelot, 'Nuclear Hyperfine Interactions in Nonlinear Semi-rigid Molecules I. The Molecular Hamiltonian', *Mol. Phys.*, **45**(5), 949–970 (1982).
5. F. Michelot, 'Nuclear Hyperfine Interactions in Nonlinear Semi-rigid Molecules II. The Effective Hamiltonian for a Non-degenerate Electronic State', *Mol. Phys.*, **45**(5), 971–1001 (1982).
6. A.E. Hansen, T.D. Bouman, 'Localized Orbital/Local Origin Method for Calculation and Analysis of NMR Shieldings. Applications to ^{13}C Shielding Tensors', *J. Chem. Phys.*, **82**(11), 5035–5047 (1985).

7. W. Kutzelnigg, U. Fleischer, M. Schindler, 'Ab Initio Calculation and Interpretation of Chemical Shifts in NMR by Means of the IGLO Method', *NMR Basic Principles and Prog.*, **23**, 165–262 (1990).
8. K. Wolinski, J.F. Hinton, P. Pulay, 'Efficient Implementation of the Gauge-independent Atomic Orbital Method for NMR Chemical Shift Calculations', *J. Am. Chem. Soc.*, **112**(23), 8251–8260 (1990).
9. T.A. Keith, R.F.W. Bader, 'Calculation of Magnetic Response Properties Using Atoms in Molecules', *Chem. Phys. Lett.*, **194**(1–2), 1–8 (1992).
10. J. Geertsen, 'A Solution of the Gauge-origin Problem for the Magnetic Shielding Constant', *Chem. Phys. Lett.*, **179**(5–6), 479–482 (1991).
11. P. Pyykkö, 'Relativistic Theory of Nuclear Spin–Spin Coupling in Molecules', *Chem. Phys.*, **22**, 289–296 (1977).
12. K. Wolinski, C.L. Hsu, J.F. Hinton, P. Pulay, 'Hartree–Fock and 2nd Order Møller–Plesset Perturbation Theory Calculations of the ^{31}P NMR Shielding Tensor in PH_3', *J. Chem. Phys.*, **99**(10), 7819–7824 (1993).
13. K. Ruud, T. Helgaker, R. Kobayashi, P. Jørgensen, K.L. Bak, H.J.A. Jensen, 'Multiconfigurational Self Consistent Field Calculations of Nuclear Shieldings Using London Atomic Orbitals', *J. Chem. Phys.*, **100**(11), 8178–8185 (1994).
14. C. van Wüllen, W. Kutzelnigg, 'Calculation of NMR Shieldings and Magnetic Susceptibilities Using Multiconfiguration Hartree–Fock Wavefunctions and Local Gauge Origins', *J. Chem. Phys.*, **104**(6), 2330–2340 (1996).
15. J. Gauss, 'Calculation of NMR Chemical Shifts at 2nd Order Many Body Perturbation Theory Using Gauge-including Atomic Orbitals', *Chem. Phys. Lett.*, **191**(6), 614–620 (1992).
16. J. Gauss, 'Effects of Electron Correlation in the Calculation of Nuclear Magnetic Resonance Chemical Shifts', *J. Chem. Phys.*, **99**(5), 3629–3643 (1993).
17. J. Gauss, 'GIAO-MBPT(3) and GIAO-SDQ-MBPT(4) Calculations of NMR Shielding Constants', *Chem. Phys. Lett.*, **229**(3), 198–203 (1994).
18. G.D. Purvis, R.J. Bartlett, 'A Full Coupled Cluster Singles and Doubles Model: The Inclusion of Disconnected Triples', *J. Chem. Phys.*, **76**(4), 1910–1918 (1982).
19. J. Gauss, J.F. Stanton, 'Coupled Cluster Calculations of NMR Chemical Shifts', *J. Chem. Phys.*, **103**(9), 3561–3577 (1995).
20. J. Gauss, J.F. Stanton, 'Perturbative Treatment of Triple Excitations in Coupled Cluster Calculations of Nuclear Magnetic Shielding Constants', *J. Chem. Phys.*, **104**(7), 2574–2583 (1996).
21. A. Barszczewicz, T. Helgaker, M. Jaszunski, P. Jørgensen, K. Ruud, 'NMR Shielding Tensors and Indirect Spin–Spin Coupling Tensors in HCN, HNC, CH_3CN and CH_3NC Molecules', *J. Magn. Reson., Ser. A*, **114**(2), 212–218 (1995).
22. J. Gauss, K. Ruud, 'On the Convergence of MBPT and CC Nuclear Shielding Constants of BH Toward the Full CI Limit', *Int. J. Quantum Chem.*, **S29**, 437–442 (1995).
23. J. Geertsen, J. Oddershede, 'Second Order Polarization Propagator Calculations of Indirect Nuclear Spin–Spin Coupling Tensors in the Water Molecule', *Chem. Phys.*, **90**, 301–311 (1984).
24. J. Geertsen, J. Oddershede, 'Higher RPA and Second Order Polarization Propagator Calculations of Coupling Constants in Acetylene', *Chem. Phys.*, **104**, 67–72 (1986).
25. J. Geertsen, J. Oddershede, G.E. Scuseria, 'Spin–Spin Coupling Constants of CO and N_2', *J. Chem. Phys.*, **87**(4), 2138–2142 (1987).
26. J. Geertsen, J. Oddershede, W.T. Raynes, G.E. Scuseria, 'Nuclear Spin–Spin Coupling in the Methane Isotopomers', *J. Magn. Reson.*, **93**, 458–471 (1991).
27. S.A. Perera, H. Sekino, R.J. Bartlett, 'Coupled Cluster Calculations of Indirect Nuclear Coupling Constants: The Importance of Non-Fermi Contact Contributions', *J. Chem. Phys.*, **101**(3), 2186–2191 (1994).
28. V. Galasso, 'Ab Initio Study of the **J**(CC) Indirect Nuclear Spin–Spin Coupling Constants in Cyclobutane and Related Systems', *Chem. Phys.*, **117**, 415–420 (1987).
29. O. Vahtras, H. Agren, P. Jørgensen, H.J.Aa. Jensen, S.B. Padkjær, T. Helgaker, 'Indirect Nuclear Spin–Spin Coupling Constants from Multiconfigurational Linear Response Theory', *J. Chem. Phys.*, **96**(8), 6120–6125 (1992).
30. A. Barszczewicz, T. Helgaker, M. Jaszunski, P. Jørgensen, K. Ruud, 'Multiconfigurational Self Consistent Field Calculations of Nuclear Magnetic Resonance Indirect Spin–Spin Coupling Constants', *J. Chem. Phys.*, **101**(8), 6822–6828 (1994).
31. S. Kirpekar, H.J.Aa. Jensen, J. Oddershede, 'Correlated Calculations of Indirect Nuclear Spin–Spin Coupling Constants for XH_4 (X = Si, Ge, and Sn)', *Chem. Phys.*, **188**, 171–181 (1994).
32. H. Sekino, R.J. Bartlett, 'Nuclear Spin–Spin Coupling Constants Evaluated Using Many Body Methods', *J. Chem. Phys.*, **85**(7), 3945–3949 (1986).
33. H. Fukui, K. Miura, H. Matsuda, 'Calculation of the Nuclear Spin–Spin Coupling Constants. VI. Many Body Perturbation Theoretical Calculation of Electron Correlation Effect', *J. Chem. Phys.*, **94**(1), 533–536 (1991).
34. R.G. Parr, W. Yang, *Density Functional Theory of Atoms and Molecules*, Oxford University Press, Oxford, 1989.
35. G. Vignale, M. Rasolt, 'Density Functional Theory in Strong Magnetic Fields', *Phys. Rev. Lett.*, **59**(20), 2360–2363 (1987).
36. G. Vignale, M. Rasolt, 'Current- and Spin-density Functional Theory for Inhomogeneous Electronic Systems in Strong Magnetic Fields', *Phys. Rev. B*, **37**(18), 10685–10696 (1988).

For references see page •••

37. G. Vignale, M. Rasolt, D.J.W. Geldart, 'Magnetic Fields and Density Functional Theory', *Adv. Quantum Chem.*, **21**, 235–253 (1990).
38. A.M. Lee, N.C. Handy, S.M. Colwell, 'The Density Functional Calculation of Nuclear Shielding Constants Using London Atomic Orbitals', *J. Chem. Phys.*, **103**(23), 10095–10109 (1995).
39. C.J. Grayce, R.A. Harris, 'Magnetic Field Density Functional Theory', *Phys. Rev. A*, **50**(4), 3089–3095 (1994).
40. C.J. Grayce, R.A. Harris, 'Two Dipole Magnetic Field Density Functional Theory', *J. Phys. Chem.*, **99**(9), 2724–2726 (1995).
41. V.G. Malkin, O.L. Malkina, M.E. Casida, D.R. Salahub, 'NMR Shielding Tensors Calculated with a Sum Over States Density Functional Perturbation Theory', *J. Am. Chem. Soc.*, **116**(13), 5898–5908 (1994).
42. V.G. Malkin, O.L. Malkina, L.A. Eriksson, D.R. Salahub, in 'Modern Density Functional Theory: A Tool for Chemistry', of *Theoretical and Computational Chemistry*, eds. P. Politzer, J.M. Seminario, Elsevier, Amsterdam, 273, Vol. 2, 1995.
43. C. van Wüllen, 'Density Functional Calculation of NMR Chemical Shifts', *J. Chem. Phys.*, **102**(7), 2806–2811 (1995).
44. A.D. Becke, 'Density Functional Thermochemistry. III. The Role of Exact Exchange', *J. Chem. Phys.*, **98**(7), 5648–5652 (1993).
45. C. Lee, W. Yang, R.G. Parr, 'Development of the Colle-Salvetti Correlation-Energy Formula into a Functional of the Electron Density', *Phys. Rev. B*, **37**(2), 785–789 (1988).
46. G. Schreckenbach, T. Ziegler, 'Calculation of NMR Shielding Tensors Using Gauge Including Atomic Orbitals and Modern Density Functional Theory', *J. Phys. Chem.*, **99**(2), 606–611 (1995).
47. G. Schreckenbach, R.M. Dickson, Y. Ruiz-Morales, T. Ziegler, in *Density Functional Theory in Chemistry*, eds. B. Laird, R. Ross, T. Ziegler, American Chemical Society, Washington, DC, 1996.
48. G. Rauhut, S. Puyear, K. Wolinski, P. Pulay, 'Comparison of NMR Shieldings Calculated from Hartree–Fock and Density Functional Wavefunctions Using Gauge-including Atomic Orbitals', *J. Phys. Chem.*, **100**(15), 6310–6316 (1996).
49. J.R. Cheeseman, G.W. Trucks, T.A. Keith, M.J. Frisch, 'A Comparison of Models for Calculating Nuclear Magnetic Resonance Shielding Tensors', *J. Chem. Phys.*, **104**(14), 5497–5509 (1996).
50. G. Schreckenbach, Y. Ruiz-Morales, T. Ziegler, 'The Calculation of ^{77}Se Chemical Shifts Using Gauge-including Atomic Orbitals and Density Functional Theory', *J. Chem. Phys.*, **104**(21), 8605–8612 (1996).
51. T.A. Keith, R.F.W. Bader, 'Calculation of Magnetic Response Properties Using a Continuous Set of Gauge Transformations', *Chem. Phys. Lett.*, **210**(1–3), 223–231 (1993).
52. O.L. Malkina, D.R. Salahub, V.G. Malkin, 'Nuclear Magnetic Resonance Spin–Spin Coupling Constants from Density Functional Theory: Problems and Results', *J. Chem. Phys.*, **105**(19), 8793–8800 (1996).
53. W. Kutzelnigg, E. Ottschofski, R. Franke, 'Relativistic Hartree–Fock by Means of Stationary Direct Perturbation Theory. 1. General Theory', *J. Chem. Phys.*, **102**(4), 1740–1751 (1995).
54. H. Nakatsuji, M. Hada, H. Kaneko, C.C. Ballard, 'Relativistic Study of Nuclear Magnetic Shielding Constants – Mercury Dihalides', *Chem. Phys. Lett.*, **255**(1–3), 195–202 (1996).
55. H. Nakatsuji, T. Nakajima, M. Hada, H. Takashima, S. Tanaka, 'Spin–Orbit Effect on the Magnetic Shielding Constants Using the Ab Initio UHF Method – Silicon Tetrahalides', *Chem. Phys. Lett.*, **247**(4–6), 418–424 (1995).
56. C.J. Jameson, J. Mason, 'The Chemical Shift', in *Multinuclear NMR*, ed. J. Mason, Plenum, New York, 51–88, 1987.
57. H. Nakatsuji, H. Takashima, M. Hada, 'Spin–Orbit Effect on the Magnetic Shielding Constant Using the Ab Initio UHF Method', *Chem. Phys. Lett.*, **233**(1–2), 95–101 (1995).
58. H. Takashima, M. Hada, H. Nakatsuji, 'Spin–Orbit effect on the Magnetic Shielding Constant Using the Ab Initio UHF Method – Ga and In Tetrahalides', *Chem. Phys. Lett.*, **235**(1–2), 13–16 (1995).
59. W. Kutzelnigg, 'Origin and Meaning of the Fermi Contact Interaction', *Theor. Chim. Acta*, **73**, 173–200 (1988).
60. G.A. Aucar, J. Oddershede, 'Relativistic Theory for Indirect Nuclear Spin–Spin Couplings within the Polarization Propagator Approach', *Int. J. Quantum Chem.*, **47**, 425–435 (1993).
61. P. Pyykkö, J.R. Wiesenfeld, 'Relativistically Parameterized Extended Hückel Calculations IV. Nuclear Spin–Spin Coupling Tensors for Main Group Elements', *Mol. Phys.*, **43**(3), 557–580 (1981).
62. C.J. Jameson, 'Theoretical and Physical Aspects of Nuclear Shielding', in *Nuclear Magnetic Resonance*, ed. G.A. Webb, Royal Society of Chemistry, London, 469–487, Vol. 26, 1997.
63. C. van Wüllen, 'Magnetic Properties of the BH Molecule – a CASSCF Study', *Theor. Chim Acta*, **87**(1–2), 89–95 (1993).
64. J. Gauss, 'Accurate Calculation of NMR Chemical Shifts', *Ber. Bunsenges. Phys. Chem.*, **99**(8), 1001–1008 (1995).
65. A.K. Jameson, C.J. Jameson, 'Gas Phase ^{13}C Chemical Shifts in the Zero-Pressure Limit. Refinements to the Absolute Shielding Scale for ^{13}C', *Chem. Phys. Lett.*, **134**(5), 461–466 (1987).
66. D.M. Grant, J.C. Facelli, D.W. Alderman, M.H. Sherwood, 'Carbon-13 Chemical Shielding Tensors in Sugars: Sucrose and Methyl-(-D-Glucopyranoside)', in

Nuclear Magnetic Shielding and Molecular Structure, ed., J.A. Tossell, Kluwer Academic Publishers, Dordrecht, 367–384, 1993.

67. F. Liu, C.G. Phung, D.W. Alderman, D.M. Grant, 'Carbon-13 Chemical Shift Tensors in Methyl Glycosides, Comparing Diffraction and Optimized Structures with Single-Crystal NMR', *J. Am. Chem. Soc.*, **118**(43), 10629–10634 (1996).
68. J.C. Facelli, D.M. Grant, 'Determination of Molecular Symmetry in Crystalline Naphthalene Using Solid State NMR', *Nature*, **365**, 325–327 (1993).
69. A.C. de Dios, D.D. Laws, E. Oldfield, 'Predicting ^{13}C NMR Chemical Shielding Tensors in Zwitterionic L-Threonine and L-Tyrosine via Quantum Chemistry', *J. Am. Chem. Soc.*, **116**(17), 7784–7786 (1994).
70. M. Kaupp, O.L. Malkina, V.G. Malkin, 'The Calculation of ^{17}O Chemical Shielding in Transition Metal Oxo Complexes. I. Comparison of DFT and Ab Initio Approaches, and Mechanisms of Relativity-induced Shielding', *J. Chem. Phys.*, **106**(22), 9201–9212 (1997).
71. M. Kaupp, 'Analysis of ^{13}C and ^{17}O Chemical Shift Tensors and ELF View of Bonding in $Fe_2(CO)_9$ and $Rh_6(CO)_{16}$', *Chem. Ber.*, **129**, 527–533 (1996).
72. Y. Ruiz-Morales, G. Schreckenbach, T. Ziegler, 'Theoretical Study of ^{13}C and ^{17}O NMR Shielding Tensors in Transition Metal Carbonyl Based on Density Functional Theory and Gauge Including Atomic Orbitals', *J. Phys. Chem.*, **100**(9), 3359–3367 (1996).
73. M.A. Fedotov, O.L. Malkina, V.G. Malkin, '$^{35/37}Cl$ NMR Chemical Shifts and Nuclear Quadrupole Couplings for Some Small Chlorine Compounds: Experimental and Theoretical Study', *Chem. Phys. Lett.*, **258**, 330–335 (1996).
74. D.B. Chesnut, E.F.C. Byrd, 'The Inclusion of Correlation in the Calculation of Phosphorus NMR Chemical Shieldings', *Heteroatom Chem.*, **7**(5), 307–312 (1996).
75. C.J. Jameson, A.K. Jameson, 'Concurrent ^{19}F and ^{77}Se or ^{19}F and ^{125}Te NMR T_1 Measurements for Determination of ^{77}Se and ^{125}Te Absolute Shielding Scales', *Chem. Phys. Lett.*, **135**(3), 254–259 (1987).
76. M. Bühl, J. Gauss, J.F. Stanton, 'Accurate Computations of ^{77}Se NMR Chemical Shifts Using the GIAO-CCSD Method', *Chem. Phys. Lett.*, **241**(3), 248–252 (1995).
77. C.J. Jameson, 'Theoretical and Physical Aspects of Nuclear Shielding', in *Nuclear Magnetic Resonance*, ed. G.A. Webb, Royal Society of Chemistry, London, 39–82, Vol. 25, 1996.
78. Y. Ruiz-Morales, G. Schreckenbach, T. Ziegler, 'Calculation of ^{125}Te Chemical Shifts Using Gauge Including Atomic Orbitals and Density Functional Theory', *J. Phys. Chem.*, **101**(22), 4121–4127 (1997).
79. G. Schreckenbach, T. Ziegler, 'Calculation of NMR Shielding Tensors Based on Density Functional Theory and a Scalar Relativistic Pauli-type Hamiltonian. The Application to Transition Metal Complexes', *Int. J. Quantum Chem.*, **61**, 899–918 (1997).
80. P.D. Ellis, J.D. Odom, A.S. Lipton, Q. Chen, J.M. Gulick, 'Gas Phase Measurements and Ab Initio Calculations of ^{77}Se and ^{113}Cd Chemical Shifts', in *Nuclear Magnetic Shielding and Molecular Structure*, ed. J.A. Tossell, Kluwer Academic, Dordrecht, 539–555, 1993.
81. T. Higashioji, M. Hada, M. Sugimoto, H. Nakatsuji, 'Basis Set Dependence of Magnetic Shielding Constant Calculated by the Hartree–Fock/Finite Perturbation Method', *Chem. Phys.*, **203**, 159–175 (1996).
82. G.E. Scuseria, 'A Systematic Study of the Ab Initio Diamagnetic Spin–Orbital Contribution to Calculated Spin–Spin Coupling Constants', *Chem. Phys.*, **107**, 417–427 (1986).
83. R.M. Dickson, T. Ziegler, 'NMR Spin–Spin Coupling Constants from Density Functional Theory with Slater-type Basis Functions', *J. Phys. Chem.*, **100**(13), 5286–5290 (1996).
84. O. Vahtras, H. Agren, P. Jørgensen, T. Helgaker, H.J.Aa. Jensen, 'The Nuclear Spin–Spin Coupling in N_2 and CO', *Chem. Phys. Lett.*, **209**(3), 201–206 (1993).
85. J. Geertsen, J. Oddershede, G.E. Scuseria, 'Calculation of Spectra and Spin–Spin Coupling Constants Using a Coupled Cluster Polarization Propagator Method', *Int. J. Quantum Chem. Symp.*, **21**, 475–485 (1987).
86. H. Fukui, K. Miura, H. Matsuda, T. Baba, 'Calculation of Nuclear Spin–Spin Couplings. VII. Electron Correlation Effects on the Five Coupling Mechanisms', *J. Chem. Phys.*, **97**(4), 2299–2304 (1992).
87. V.G. Malkin, O.L. Malkina, D.R. Salahub, 'Calculations of Spin–Spin Coupling Constants Using Density Functional Theory', *Chem. Phys. Lett.*, **221**(1–2), 91–99 (1994).
88. S.A. Perera, M. Nooijen, R.J. Bartlett, 'Electron Correlation Effects on the Theoretical Calculation of Nuclear Magnetic Resonance Spin–Spin Coupling Constants', *J. Chem. Phys.*, **104**(9), 3290–3305 (1996).
89. A. Barszczewicz, M. Jaszunski, K. Kamienska-Trela, T. Helgaker, P. Jørgensen, O. Vahtras, 'Ab Initio Study of the NMR Shielding Constants and Spin–Spin Coupling Constants in Cyclopropene', *Theor. Chim. Acta*, **87**, 19–28 (1993).
90. V. Galasso, 'Theoretical Study of Spectroscopic Properties of Cubane', *Chem. Phys.*, **184**, 107–114 (1994).
91. C.J. Jameson, J. Mason, 'Spin–Spin Coupling' in *Multinuclear NMR*, ed., J. Mason, Plenum, New York, 89–132, 1987.
92. M.D. Lumsden, K. Eichele, R.E. Wasylishen, T.S. Cameron, J.F. Britten, 'Determination of a $^{199}Hg–^{31}P$ Indirect Spin–Spin Coupling Tensor via Single-crystal Phosphorus NMR Spectroscopy', *J. Am. Chem. Soc.*, **116**(24), 11129–11136 (1994).
93. M. Karplus, 'Contact Electron Spin Coupling of Nuclear Magnetic Moments', *J. Chem. Phys.*, **30**(1), 11–15 (1959).
94. H. Fukui, H. Inomata, T. Baba, K. Miura, H. Matsuda, 'Calculation of Nuclear Spin–Spin Couplings. VIII.

For references see page •••

Vicinal Proton–Proton Coupling Constants in Ethane', *J. Chem. Phys.*, **103**(15), 6597–6600 (1995).
95. G. Breit, 'Possible Effects of Nuclear Spin on X-Ray Terms', *Phys. Rev.*, **35**(12), 1447–1451 (1930).
96. P. Pyykkö, E. Pajanne, M. Inokuti, 'Hydrogen Like Relativistic Corrections for Electric and Magnetic Hyperfine Integrals', *Int. J. Quantum Chem.*, **7**, 785–806 (1973).
97. K.E. Vermillion, P. Florian, P.J. Grandinetti, 'Relationships Between Bridging Oxygen ^{17}O Quadrupolar Coupling Parameters and Structure in Alkali Silicates', *J. Chem. Phys.*, **108**(17), 7274–7285 (1998).
98. C. Müller, W. Schajor, H. Zimmermann, U. Haeberlen, 'Deuteron Chemical Shift and EFG Tensor in α-Glycine', *J. Magn. Reson.*, **56**, 235–246 (1984).
99. P.L. Cummins, G.B. Bacskay, N.S. Hush, 'The Prediction of Nuclear Quadrupole Moments from Ab Initio Quantum Chemical Studies on Small Molecules. II. The Electric Field Gradients at the ^{17}O, ^{35}Cl, and ^{2}H Nuclei in CO, NO^+, OH^-, H_2O, CH_2O, HCl, LiCl, and FCl', *J. Chem. Phys.*, **87**(1), 416–423 (1987).
100. R. Ludwig, F. Weinhold, T.C. Farrar, 'Experimental and Theoretical Studies of Hydrogen Bonding in Neat, Liquid Formamide', *J. Chem. Phys.*, **102**(13), 5118–5125 (1995).
101. B.F. King, T.C. Farrar, F. Weinhold, 'Quadrupole Coupling Constants in Linear $(HCN)_n$ clusters: Theoretical and Experimental Evidence for Cooperativity Effects in C–H···N Hydrogen Bonding', *J. Chem. Phys.*, **103**(1), 348–352 (1995).
102. W.P. Power, R.E. Wasylishen, 'NMR Studies of Isolated Spin Pairs in the Solid State', in *Annual Reports on NMR Spectroscopy*, ed., G.A. Webb, Academic Press, London, Vol. 23, 1–84, 1991.
103. P. Zhang, C. Dunlap, P. Florian, P.J. Grandinetti, I. Farnan, J.F. Stebbins, 'Silicon Site Distributions in an Alkali Silicate Glass Derived by Two-dimensional ^{29}Si NMR', *J. Non. Cryst. Solids*, **204**, 294–300 (1996).
104. I. Farnan, P.J. Grandinetti, J.H. Baltisberger, J.F. Stebbins, U. Werner, M.A. Eastman, A. Pines, 'Quantification of the Disorder in Network-modified Silicate Glasses', *Nature*, **358**, 31–35 (1992).
105. A.C. de Dios, C.J. Jameson, 'The NMR Chemical Shift: Insight into Structure and Environment', in *Annual Reports on NMR Spectroscopy*, ed., G.A. Webb, Academic Press, London, 1–69, Vol. 29, 1994.
106. A.C. de Dios, J.G. Pearson, E. Oldfield, 'Secondary and Tertiary Structural Effects on Protein NMR Chemical Shifts: An ab Initio Approach', *Science*, **260**, 1491–1496 (1993).
107. A.C. de Dios, E. Oldfield, 'Ab Initio Study of the Effects of Torsion Angles on Carbon-13 Nuclear Magnetic Resonance Chemical Shielding in *N*-Formyl-L-Alanine, *N*-Formyl-L-Valine Amide, and Some Simple Model Compounds: Applications to Protein NMR Spectroscopy', *J. Am. Chem. Soc.*, **116**(12), 5307–5314 (1994).
108. H.B. Le, J.G. Pearson, A.C. de Dios, E. Oldfield, 'Protein Structure Refinement and Prediction via NMR Chemical Shifts and Quantum Chemistry', *J. Am. Chem. Soc.*, **117**(13), 3800–3807 (1995).
109. C.J. Jameson, A.C. de Dios, 'The Nuclear Shielding Surface: The Shielding as a Function of Molecular Geometry and Intermolecular Separation', in *Nuclear Magnetic Shielding and Molecular Structure*, ed. J.A. Tossell, Kluwer Academic, Dordrecht, 95–116, 1993.
110. C.J. Jameson, 'Understanding NMR Chemical Shifts', *Ann. Rev. Phys. Chem.*, **47**, 135–169 (1996).
111. C.J. Jameson, 'Rovibrational Averaging of Molecular Electronic Properties', in *Theoretical Models of Chemical Bonding*, Part 3. Molecular Spectroscopy, Electronic Structure, and Intramolecular Interactions, ed. Z.B. Maksic, Springer-Verlag, Berlin, 457–519, 1991.
112. W.T. Raynes, 'Theory of Vibrational Effects on Properties of Methane and its Isotopomers. The Polarizability, Magnetizability, Carbon-13 Shielding and the One- and Two-bond Spin–Spin Coupling Constants', *Mol. Phys.*, **63**(4), 719–729 (1988).
113. J. Geertsen, J. Oddershede, W.T. Raynes, T.L. Marvin, 'Accurate Ab Initio Carbon–Proton and Proton–Proton Spin–Spin Coupling Surfaces for the Methane Molecule', *Mol. Phys.*, **82**(1), 29–50 (1994).
114. W.T. Raynes, J. Geertsen, J. Oddershede, 'Nuclear Spin–Spin Coupling and Nuclear Motion', *Int. J. Quantum Chem.*, **52**(1), 153–163 (1994).
115. B. Bennett, W.T. Raynes, C.W. Anderson, 'Temperature Dependence of J(CH) and J(CD) in $^{13}CH_4$ and some of its Isotopomers', *Spectrochim. Acta A*, **45**(8), 821–827 (1989).
116. A.C. de Dios, C.J. Jameson, 'The ^{129}Xe Nuclear Shielding Surfaces for Xe Interacting with Linear Molecules CO, N_2 and CO_2', *J. Chem. Phys.*, **107**(11), 4253–4270 (1997).
117. C.J. Jameson, H.M. Lim, A.K. Jameson, 'The Role of Polarization of Xe by Di- and Monovalent Cations in ^{129}Xe NMR Studies in Zeolite A', *Solid State Nucl. Magn. Reson.*, **9**, 277–301 (1997).
118. J.F. Hinton, P. Guthrie, P. Pulay, K. Wolinski, 'Ab Initio Quantum Mechanical Calculation of the Chemical Shift Anisotropy of the Hydrogen Atom in the $(H_2O)_{17}$ Cluster', *J. Am. Chem. Soc.*, **114**(5), 1604–1605 (1992).
119. T.B. Woolf, V.G. Malkin, O.L. Malkina, D.R. Salahub, B. Roux, 'The Backbone ^{15}N chemical shift Tensor of the Gramicidin Channel. A Molecular Dynamics and Density Functional Study', *Chem. Phys. Lett.*, **239**, 186–194 (1995).
120. C.J. Jameson, H.-M. Lim, 'Ab Initio Studies of the Nuclear Magnetic Resonance Chemical Shifts of a Rare Gas Atom in a Zeolite', *J. Chem. Phys.*, **103**(10), 3885–3894 (1995).
121. C.J. Jameson, A.K. Jameson, B.I. Baello, H.M. Lim, 'Grand Canonical Monte Carlo Simulations of Xenon in

Zeolite NaA, I. Distribution and ^{129}Xe Chemical Shifts', *J. Chem. Phys.*, **100**(8), 5965–5976 (1994).

122. C.J. Jameson, A.K. Jameson, R.E. Gerald II, H.-M Lim, 'Xe_n Clusters in the Alpha Cages of Zeolite KA', *J. Chem. Phys.*, **103**(20), 8811–8820 (1995).
123. C.J. Jameson, H.M. Lim, 'Distribution and ^{129}Xe Chemical Shifts of Xe_n Clusters in the Alpha Cages of Zeolite AgA', *J. Chem. Phys.*, **107**(11), 4373–4383 (1997).
124. C.J. Jameson, A.K. Jameson, R.E. Gerald II, H.M. Lim, 'Anisotropic Xe Chemical Shifts in Zeolites. The Role of Iintra- and Inter-crystallite Diffusion', *J. Phys. Chem.*, **101**(42), 8418–8437 (1997).
125. J. Sauer, J.R. Hill, 'The Acidity of Surface Silanol Groups. A Theoretical Estimate Based on Ab Initio Calculations on a Model Surface', *Chem. Phys. Lett.*, **218**, 333–337 (1994).
126. F. Haase, J. Sauer, 'Interaction of Methanol with Brønsted Acid Sites of Zeolite Catalysts: An Ab Initio Study', *J. Am. Chem. Soc.*, **117**(13), 3780–3789 (1995).

For references see page •••